

冀北大滩盆地钾玄岩系列的厘定、 岩石成因及与铀成矿关系

高天栋¹⁾, 郭恒飞¹⁾, 姜山¹⁾, 巫建华²⁾, 牛子良¹⁾,
王洪志¹⁾, 王之晟¹⁾, 马国祥¹⁾

1) 核工业二四三大队, 内蒙古赤峰 024000;
2) 东华理工大学核资源与环境国家重点实验室, 南昌, 330013



内容提要: 大滩盆地位于华北克拉通北缘隆起带和沽源—红山子铀成矿带西南段, 盆地内五里营铀矿点赋存在义县期(早白垩世晚期)二长斑岩中。二长斑岩全岩为高钾、富碱、低钛、贫铁, 富集轻稀土元素和大离子亲石元素, 无明显 Eu 负异常, 具有碱性系列和钙碱性系列的特征, 属典型的钾玄岩系列; $[n(^{87}\text{Sr})/n(^{86}\text{Sr})]_i$ 为 0.707290~0.707399 (平均值为 0.707343), $[n(^{143}\text{Nd})/n(^{144}\text{Nd})]_i$ 为 0.511849~0.511895 (平均值为 0.511876), $\varepsilon_{\text{Nd}}(t)$ 值变化范围是 -12.38~-11.49, $[n(^{206}\text{Pb})/n(^{204}\text{Pb})]_i$ 为 17.236~17.343 (平均值为 17.296), $[n(^{207}\text{Pb})/n(^{204}\text{Pb})]_i$ 为 15.407~15.428 (平均值为 15.416), $[n(^{208}\text{Pb})/n(^{204}\text{Pb})]_i$ 为 37.666~37.707 (平均值为 37.684)。 $\varepsilon_{\text{Nd}}(t)$ — $[n(^{87}\text{Sr})/n(^{86}\text{Sr})]_i$ 、 $[n(^{143}\text{Nd})/n(^{144}\text{Nd})]_i$ — $[n(^{87}\text{Sr})/n(^{86}\text{Sr})]_i$ 、 $[n(^{207}\text{Pb})/n(^{204}\text{Pb})]_i$ — $[n(^{206}\text{Pb})/n(^{204}\text{Pb})]_i$ 和 $[n(^{208}\text{Pb})/n(^{204}\text{Pb})]_i$ — $[n(^{206}\text{Pb})/n(^{204}\text{Pb})]_i$ 图解显示岩浆来源与 EM I 富集地幔密切相关, 可能还有下地壳组分的参与。受太平洋板块洋壳俯冲和华北克拉通岩石圈拆沉的双重影响, 其构造环境为拉伸环境, 岩浆主要源于加厚陆壳底部物质的部分熔融。五里营铀矿化与下庄矿田“交点型”铀矿床成矿特征相似, 赋存于一系列 NNW 向硅化、青磐岩化蚀变带内, 其赋矿围岩二长斑岩(钾玄岩系列)所具备的富集地幔印记制约着 U 等大离子亲石元素的富集。

关键词: 钾玄岩系列; EM I 富集地幔; 构造环境; 铀成矿; 大滩盆地

钾玄岩系列(Shoshonite series)火山岩是一套产于特定构造地质环境、具有独特岩石学和地球化学特征的富钾中(基)性火山岩系, 包括基性的 absarokite(钾质粗面玄武岩), 中性的 shoshonite(钾玄岩)和中酸性的 banakite/latite(安粗岩)(邱家骧等, 1991); 章邦桐等(2011a)建议分别译为粗玄岩、玄粗岩和安粗岩。钾玄岩系列为一套与碱性橄榄玄武岩系列、拉斑玄武岩系列及钙碱性系列并列的、独立的火山岩组合(Moirson, 1980; Liegeois, 1998; Peccerillo, 1999, 2001; Sun C H and Stern R J, 2001)。Morrison(1980)总结了钾玄岩系系列岩石化学特征, 主要包括: ①基性岩中 SiO_2 接近饱和, 很少有标准矿物霞石或石英; ②铁的富集程度较碱性橄榄玄武岩低; ③全碱含量高 ($\text{Na}_2\text{O} + \text{K}_2\text{O} > 5\%$); ④高的 $\text{K}_2\text{O}/\text{Na}_2\text{O}$ 值, $\text{SiO}_2 = 50\%$ 时, 该值 > 0.6 ; $\text{SiO}_2 = 55\%$

时, 该值 > 1.0 ; ⑤ $\text{K}_2\text{O}-\text{SiO}_2$ 图解在低 SiO_2 的区域, 呈现陡的正倾斜, $\text{SiO}_2 > 57\%$ 时, 斜率为零或负; ⑥高的 $\text{Fe}_2\text{O}_3/\text{FeO}$ 比值 (> 0.5); ⑦低的 TiO_2 ($< 1.3\%$); ⑧高而多变的 Al_2O_3 , 含量为 $14\% \sim 19\%$; ⑨富集 P、Rb、Sr、Ba、Pb 和轻稀土元素, 与钾的富集一致。橄榄玄粗岩系主要发育于岛弧区(Morrison G, 1980)、活动大陆边缘、裂谷带及地缝合线两侧(Varne, 1985; Thompson, 1985)等特殊构造环境, 与金—铜—铀矿化有着一定联系(John et al., 2002; 张运涛等, 2013; 邓晋福等, 2015)。自 20 世纪 90 年代起, 我国东部的中生代额尔古纳火山—侵入岩带(许文良等, 1994)、燕山—辽西火山—侵入岩带(廖群安等, 1993; 鲍亦冈等, 1995)、长江中下游火山—侵入岩带(赵太平等, 1994; 薛怀民等, 1989)、江西峡江—广丰火山岩带(廖群安等, 1999)陆续有钾玄岩系列报道, 之后, 钾玄岩系列的厘定、特征研究和成因探讨

注: 本文为中国核工业地质局铀资源调查评价项目(编号: 201933-4)的成果。

收稿日期: 2022-03-16; 改回日期: 2022-08-11; 网络首发: 2022-08-20; 责任编辑: 章雨旭。Doi: 10.16509/j.georeview.2022.08.045

作者简介: 高天栋, 男, 1967 年生, 本科, 高级工程师, 主要从事铀矿勘查和研究; Email: gtd243@163.com。

成为我国地质工作者的研究热点(章邦桐等,2008,2011b;张双涛等,2005;李毅等,2006;祝禧艳和巫建华,2007;贺振宇等,2008;吴俊奇等,2011;薛怀民等,2015;项媛馨等,2012;王佳玲和巫建华,2014;巫建华等,2014a)。

近年来在沽源—红山子铀成矿带南部的大滩盆地五里营地区新发现了一批铀矿点、铀异常点,其铀矿化、异常主要赋存于义县期中基性潜火山岩中,地质时代属早白垩世晚期①,明显不同于该成矿带已知的赋矿层位—早白垩世早期张家口组高钾钙碱性流纹岩—碱性粗面岩组合(姜山等,2011;朱凤丽,

2012;巫建华等,2014b,2015,2017a,2017b;孟艳宁等,2015;夏应冰等,2016;张雅菲等,2016)和晚侏罗世早期新民组高钾钙碱性—碱性流纹岩组合中(巫建华等,2013,2014b,2016,2017b;祝洪涛等,2014;解开瑞等,2016;黎伟等,2017;宋凯等,2017),但是,目前该赋矿层位的基础研究十分薄弱,仍缺少系统的岩性—岩相学、地球化学特征及岩石成因方面的研究,因此,本文选择大滩盆地五里营铀矿点赋矿围岩作为研究对象,通过镜下鉴定、元素和 Sr—Nd—Pb 同位素示踪技术厘定其岩石系列,并探讨岩石成因,为深入研究该地区的铀成矿机制和下一步找矿

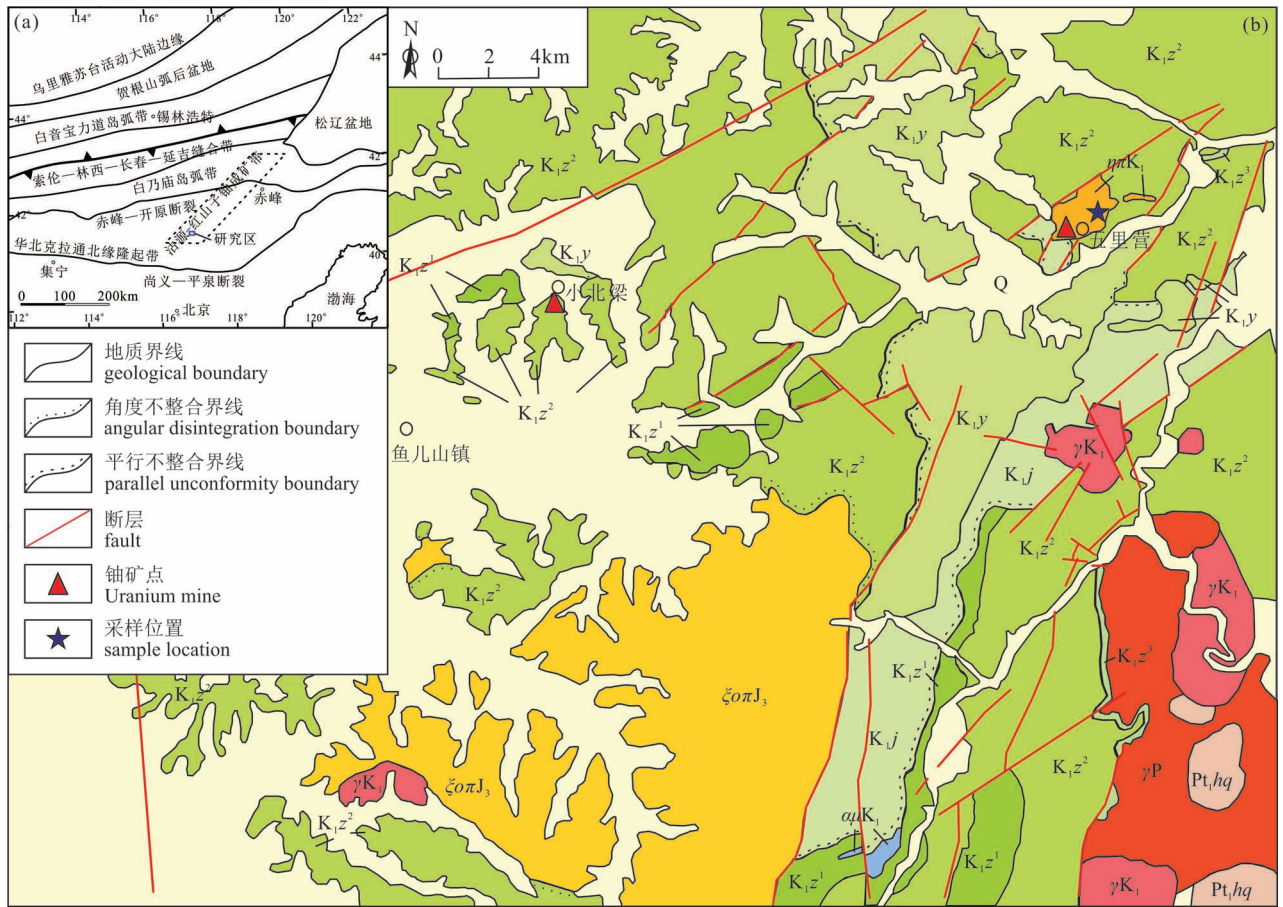


图 1 冀北大滩盆地大地构造位置(a) (据 Zhang Shuanhong et al., 2014)及地质简图(b) (据张雅菲等, 2016)

Fig. 1 Geotectonic (a) (after Zhang Shuanhong et al., 2014) and geological (b) (after Zhang Yafei et al., 2016&) sketch map of the Datun Basin, northern Hebei

Q—第四系;K_{1j}f—下白垩统九佛堂组;K_{1y}—下白垩统义县组;下白垩统张家口组: K_{1z}³—三段, K_{1z}²—二段, K_{1z}¹—一段; Pt₁hq—古元古界红旗营子群;αK₁—早白垩世安山玢岩;ηK₁—早白垩世二长斑岩;ξOJ₃—晚侏罗世石英正长斑岩; γK₁—早白垩世花岗岩;γP—二叠纪花岗岩

Q—Quaternary; K_{1j}f—Lower Cretaceous Jiufotang Formation; K_{1y}—Lower Cretaceous Yixian Formation; Lower Cretaceous Zhangjiakou Formation: K_{1z}³—the Third Member of, K_{1z}²—the Second Member, K_{1z}¹—the First Member; Pt₁hq—Palaeoproterozoic Hongqiyingzi Group; αK₁—Early Cretaceous andesitic porphyrite; ηK₁—Early Cretaceous ivernite; ξOJ₃—Late Jurassic feldspar porphyritic granite; γK₁—Early Cretaceous granite; γP—Permian granite

工作奠定基础。

1 地质概况

大滩盆地位于河北省承德市丰宁满族自治县北部,大地构造位置处于华北克拉通北缘隆起带和沽源—红山子铀成矿带西南部(图1a),盆地具有“基底+盖层”二元结构特征,基底以古元古界红旗营子群变质岩系和海西期花岗岩为主,红旗营子群主要由黑云母变粒岩、浅粒岩、石英岩和大理岩组成(巫建华等,2015);盖层主要为下白垩统热河群与张家口组火山岩系(图1b)。热河群以含煤碎屑岩—中基性火山岩组合为特征,包括九佛堂组和义县组,前者为一套黑色纸片状页岩、泥岩、泥质粉砂岩,后者为一套以中、基性为主局部夹中酸性、碱性的火山岩、火山碎屑岩及沉积岩,LA-ICP-MS 锆石 U-Pb 年龄为 127.7~114.9 Ma(陈井胜等,2015,牛子良等,2016);张家口组分布较广且厚度巨大,可划分为三个岩性段,下段主要是以流纹岩为主,其次为流纹质

熔结角砾岩、角砾凝灰岩和熔结凝灰岩夹流纹岩;中段主要是以中性粗面岩为主,其次为粗面岩和石英粗面岩,中间夹少量流纹岩;上段以酸性熔岩和火山碎屑岩为主夹火山碎屑沉积岩。

盆地断裂划分为 NE(NNE)、NW、近 EW、近 SN 向等 4 组,NE 向断裂是最主要的断裂,该方向的断裂对铀及多金属矿化起着明显的控制作用。

盆地内岩浆活动强烈,发育二叠纪花岗岩、晚侏罗世石英正长斑岩以及早白垩世花岗岩、酸性、中基性潜火山岩。五里营铀矿点处的潜火山岩较为发育,呈环形沿五里营—老东营火山塌陷构造边缘分布,具体定位于断裂构造结点,尤其是 NE 向 F_{17} 、 F_{46} 断裂带与其他方向断裂复合部位。潜火山岩形态受侵位空间制约,多呈岩株状、带状岩墙、岩脉和岩枝状产出,可分为张家口期流纹斑岩和义县期安山玢岩、二长斑岩(SHRIMP 锆石 U-Pb 年龄为 $122.7 \pm 6.3 \text{Ma}^{\text{①}}$)。其中,二长斑岩呈北东宽南西窄的楔状产于 NE 与 NW 向断裂交汇处,规模 $2 \times 0.6 \text{ km}$,顶

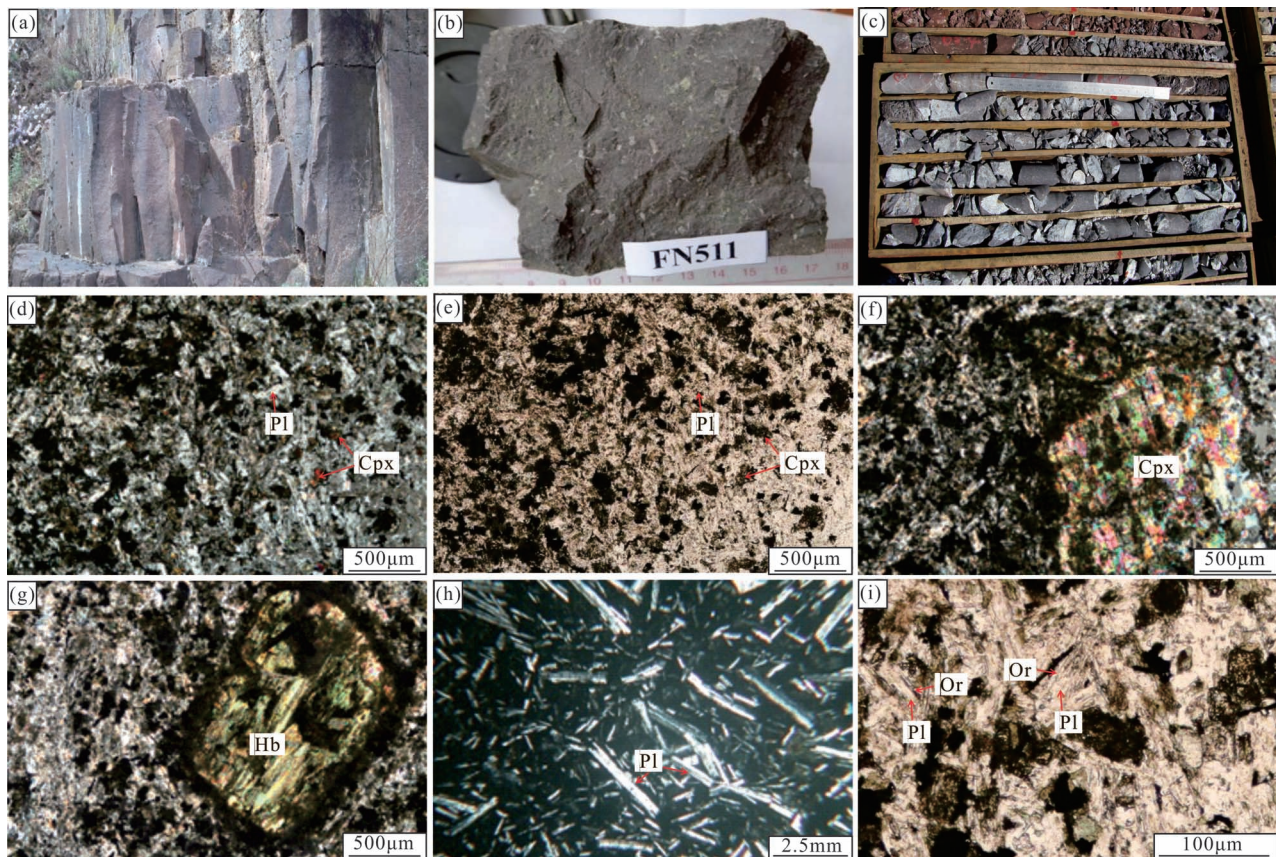


图2 冀北大滩盆地二长斑岩手标本及镜下照片

Fig. 2 Field photographs of overbite in the Datun Basin, northern Hebei

Pl—斜长石; Cpx—单斜辉石; Hb—角闪石; Or—正长石

Pl—plagioclase; Cpx—clinopyroxene; Hb—amphibole; Or—orthoclase

界面埋深 NE 浅 SW 深,岩体深部中心部位呈“V”字型岩株状产出,具有柱状节理。

2 岩相学特征

本文研究的样品取自五里营铀矿点地表和 ZK3 钻孔 210~240m 处,地表露头发育柱状节理(图 2a),岩石颜色为深灰色—灰黑色,块状构造,斑状结构(图 2b、c),斑晶主要为斜长石和少量的角闪石和单斜辉石,斑晶含量 3%~5%(图 2d、e)。其中,斜长石呈灰白色自形—半自形板柱状,含量约占斑晶的 20%,粒径 0.5~1mm。偶见 3mm 左右的斑晶,具有聚片双晶和正长石环边结构(图 2h、i);单斜辉石呈浅黄褐色他形—半自形短柱状、粒状,粒径 0.5~2mm,正高突起,多色性很弱,正光性。可见有明显的两组近于垂直的解理(图 2f);角闪石呈浅褐色半自形短柱状,粒径 1~2mm,正中高突起,具明显的多色性,边缘由微细磁铁矿和辉石组成暗化边,见一

组解理(图 2g)。基质由长柱状微晶斜长石、角闪石半定向分布夹尘土状铁质、暗色矿物及玻璃质组成交织结构(图 2h),副矿物为半自形粒状磁铁矿,斜长石具正长石环边结构(图 2i)。

可见,五里营铀矿点次火山岩斑晶以斜长石为主,含单斜辉石和角闪石。基质具有交织结构,斑晶和基质中的斜长石均可见正长石环边,具有钾玄岩系列的矿物学特征,初步定名为二长斑岩。

3 分析方法

3.1 主量与微量元素分析

样品全岩主、微量元素分析测试在核工业北京地质研究院分析测试中心完成。主量元素分析测试采用化学分析法(CA)和 X 射线荧光光谱法(XRF)。化学分析法主要分析氧化亚铁的含量,X 射线荧光光谱法在 AxiosmAX X 射线荧光光谱仪上完成,测试前的样片制作可参见周万蓬(2015),实

表 1 冀北大滩盆地二长斑岩主量元素(%)、微量元素($\times 10^{-6}$)及有关参数

Table 1 Major(%) and trace element($\times 10^{-6}$) contents of ivernite in the Datan Basin, northern Hebei

样号	FN511	FN514	FN515	FN516	FN517	样号	FN511	FN514	FN515	FN516	FN517
SiO ₂	57.9	58.5	59.1	58.7	59.0	Dy	5.79	5.92	6.39	5.71	5.14
TiO ₂	1.26	1.23	1.24	1.23	1.13	Ho	1.08	1.05	1.18	0.99	0.96
Al ₂ O ₃	16.3	16.4	16.5	16.4	16.3	Er	3.01	2.77	3.22	2.72	2.59
Fe ₂ O ₃	3.89	4.75	4.64	4.36	3.36	Tm	0.45	0.42	0.50	0.41	0.40
FeO	2.45	1.94	2.02	2.14	2.40	Yb	2.69	2.58	3.00	2.51	2.47
MnO	0.21	0.09	0.10	0.08	0.28	Lu	0.38	0.36	0.45	0.35	0.34
MgO	1.54	1.55	1.39	1.36	1.57	ΣREE	301	316	315	301	297
CaO	4.24	3.61	3.69	3.73	3.59	(La/Yb) _N	16.7	18.6	15.5	18.0	18.2
Na ₂ O	4.81	4.20	4.71	4.64	2.77	(La/Sm) _N	4.24	4.10	4.14	4.16	4.35
K ₂ O	3.61	4.23	3.96	4.05	6.21	(Gd/Yb) _N	2.45	2.65	2.39	2.70	2.54
P ₂ O ₅	0.62	0.60	0.60	0.61	0.53	δEu	0.92	0.91	0.89	0.93	0.91
烧失量	3.09	2.40	2.08	2.24	2.85	δCe	0.92	0.91	0.90	0.90	0.93
总量	99.92	99.50	100.03	99.54	99.99	Cr	1.79	2.54	1.82	1.64	1.66
Na ₂ O+K ₂ O	8.42	8.43	8.67	8.69	8.98	Co	11.2	10.6	10.5	9.77	9.89
K ₂ O/Na ₂ O	0.75	1.01	0.84	0.87	2.24	Ni	3.12	6.51	2.70	2.31	1.73
TFeO	6.13	6.36	6.32	6.20	5.58	Rb	109	145	128	133	189
Fe ₂ O ₃ /FeO	1.59	2.45	2.30	2.04	1.40	Sr	713	687	694	710	598
Mg [#]	52.8	58.7	55.1	53.1	53.8	Ba	1457	1561	1512	1503	1624
La	66.3	71.0	69.0	66.8	66.6	Th	9.94	10.8	10.5	10.7	11.2
Ce	124	129	127	123	124	U	2.41	2.43	2.39	2.31	2.88
Pr	14.9	15.7	16.0	15.5	14.7	Zr	290	301	324	302	310
Nd	60.1	64.0	64.4	60.8	58.2	Hf	7.92	8.09	8.89	8.50	8.69
Sm	9.85	10.9	10.5	10.1	9.63	Nb	23.2	23.8	23.5	23.3	22.6
Eu	2.70	2.87	2.82	2.80	2.58	Ta	1.29	1.32	1.38	1.34	1.36
Gd	8.12	8.43	8.84	8.36	7.74	Y	37.2	31.8	36.3	29.1	27.6
Tb	1.26	1.32	1.38	1.27	1.18	Ga	23.9	23.9	23.3	23.0	22.5

注:TFeO=FeO+0.89Fe₂O₃;Mg[#]=100 $\frac{n(\text{Mg})}{n(\text{Mg})+n(\text{TFeO})}$,Fe 为全铁;δEu=2 $\frac{[\text{Eu}]_{\text{N}}}{[\text{Sm}]_{\text{N}}+[\text{Gd}]_{\text{N}}}$, [Eu]_N、[Sm]_N、[Gd]_N 为相应元素的球粒

陨石标准化值。

验过程中,X射线管电压为50 kV,电流为50 mA,元素分析测试下限大于0.01%,分析相对误差小于5%,检测方法和依据参照GB/T 14506.14-2010《硅酸盐岩石化学分析方法 第14部分:氧化亚铁量测定》,GB/T 14506.28-2010《硅酸盐岩石化学分析方法 第28部分:16个主次成分量测定》,岩石矿物分析《第四版 16.20 灼烧减量的测定》。微量元素分析测试采用电感耦合等离子质谱法(ICP-MS)。样品溶液的配制过程可见参周万蓬(2015),分析测试

是在NexION 300D等离子体质谱仪上完成,工作温度控制在20℃,相对湿度保持在27%,当微量元素含量小于10 $\mu\text{g/g}$ 时,相对误差小于10%,当微量元素含量大于10 $\mu\text{g/g}$ 时,相对误差小于5%,测试方法和依据参照GB/T 14506.30-2010《硅酸盐岩石化学分析方法 第30部分:44个元素量测定》。大滩盆地二长斑岩主、微量元素分析结果列于表1。

3.2 Sr—Nd—Pb 同位素分析

样品全岩 Sr—Nd—Pb 同位素组成测试工作在

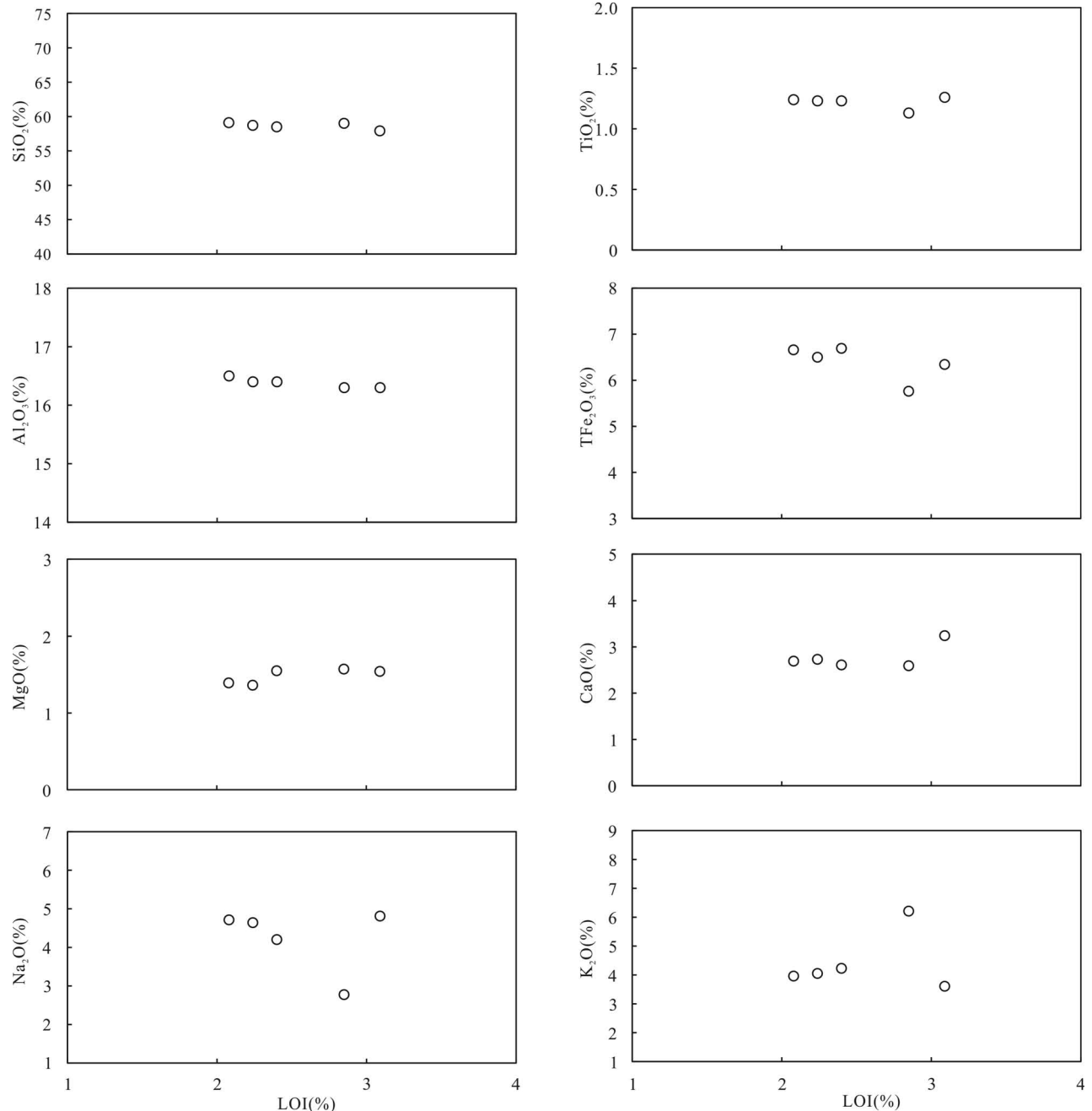


图3 冀北大滩盆地二长斑岩烧减量—主要元素二元图解

Fig. 3 Bivariate diagrams of LOI—elements of ivernite in Datun Basin, northern Hebei

核工业北京地质研究院分析测试中心完成。Sr 同位素分析测试采用 Phoenix 热表面电离质谱仪,检测方法和依据参照 EJ/T 692-1992《岩石矿物铷锶等时年龄测定》;Nd 同位素分析测试采用 ISOPROBE-T 热表面电离质谱仪,检测方法和依据参照 GB/T 17672-1999《岩石中铅、锶、钕同位素测定方法》;Pb 同位素分析测试采用 ISOPROBE-T 热表面电离质谱仪,检测方法和依据参照 DZ/T 0184.12-1997《岩石、矿物中微量铅的同位素组成的测定》。大滩盆地二长斑岩 Sr—Nd—Pb 同位素分析结果及有关参数列于表 2。

4 分析结果

牛头沟地段岩浆活动发育,热液蚀变强烈。在挑选了新鲜的岩石样品后,为保证能够有效地利用样品元素特征进行岩石分类、成因探讨(Rollinson, 1993),首先以样品烧失量(LOI)为横坐标做 Harker 图解评估岩浆演化和岩石形成过程中热液蚀变对元素特别是活动性强的元素的影响,排除受影响较大的元素。通常被认为活动性差的元素(Si、Ti、Fe),样品随蚀变程度升高它们基本能保持含量稳定, Si、Ti、Fe 均与 LOI 之间没有明显相关性(图 3),表明这些元素受热液活动的影响比较小;通常认为碱金属、碱土金属元素(Na、K、Al、Mg)具有极高的活动性,(Humphris et al., 1978), Na、K、Al、Mg 同样均与 LOI 之间没有相关性,仅样品 FN517 的 Na₂O、K₂O 有较

小的变化,但仍在正常范围内,并非热液蚀变影响(图 3),能够代表样品基本特征。

4.1 主量元素

五里营二长斑岩主量元素分析结果显示,样品的主量元素总量为 99.50%~100.03%,经百分化校正后,样品 SiO₂ 含量变化于 59.7%~60.7%之间(平均 58.6%),全碱 Na₂O+K₂O=8.63%~9.24%(平均 8.86%),表现出富碱的特征,在 TAS 图解(图 4a)上落入碱性系列的粗安岩区。为进一步消除烧失量较大导致部分活动元素的带入带出的影响,采用不活动元素构建 Zr/TiO₂—Nb/Y 图解(图 4b)讨论岩石系列,结果显示样品落入碱性系列的粗面安山岩区,指示碱性系列的特征;同时在 Ce/Yb—Ta/Yb 图解(图 5a)上均落入钾玄岩系列范围。Al₂O₃ 含量较高,变化范围为 16.76%~16.84%(平均 16.80%),TiO₂ 含量较低,变化范围为 1.16%~1.30%(平均 1.22%),K₂O=3.72%~6.39%(平均 4.41%),K₂O/Na₂O 比值高,为 0.75~2.24(平均 1.14),表现出富钾的特征,在 K₂O—SiO₂ 图解(图 5b)上落入高钾钙碱性与钾玄岩系列分界线之上,属钾玄岩系列;全铁含量较低,TFeO=5.58%~6.36%(平均 6.12%),但 Fe₂O₃/FeO 比值高,为 1.40~2.45(平均 1.95),在 AFM 图解(图 6a)上,粗安岩主要落入钙碱性系列范围。同样,考虑到样品的 K₂O 和 Na₂O 在蚀变过程中可能被带出,导致投影点偏向 F 端元,故采用 MgO—TFeO 图解讨论岩

表 2 冀北大滩盆地二长斑岩 Sr—Nd—Pb 同位素分析结果

Table 2 Sr—Nd—Pb isotopic compositions of ivernite in Datan Basin, northern Hebei

样品号	Rb ($\times 10^{-6}$)	Sr ($\times 10^{-6}$)	$\frac{n(^{86}\text{Rb})}{n(^{87}\text{Sr})}$	$n(^{87}\text{Sr})/n(^{86}\text{Sr})$		$\left[\frac{n(^{87}\text{Sr})}{n(^{86}\text{Sr})}\right]_i$	Sm ($\times 10^{-6}$)	Nd ($\times 10^{-6}$)	$\frac{n(^{147}\text{Sm})}{n(^{144}\text{Nd})}$
	测值	$\pm 1\sigma$	测值	$\pm 1\sigma$					
FN514	145	687	0.5962	0.708356	0.000012	0.707339	64.0	0.1076	10.9
FN515	128	694	0.5210	0.708178	0.000013	0.707290	64.4	0.1030	10.5
FN516	133	710	0.5291	0.708301	0.000011	0.707399	60.8	0.1050	10.1
样品号	$n(^{143}\text{Nd})/n(^{144}\text{Nd})$		$\left[\frac{n(^{143}\text{Nd})}{n(^{144}\text{Nd})}\right]_i$	$\varepsilon_{\text{Nd}}(t)$	$f_{\text{Sm}/\text{Nd}}$	T_{DM2}	U($\times 10^{-6}$)	Th($\times 10^{-6}$)	Pb($\times 10^{-6}$)
	测值	$\pm 1\sigma$							
FN514	0.511979	0.000007	0.511895	-11.49	-0.45	1847	2.43	10.8	11.7
FN515	0.511930	0.000007	0.511849	-12.38	-0.48	1918	2.39	10.5	9.26
FN516	0.511967	0.000011	0.511885	-11.69	-0.47	1862	2.31	10.7	10.2
样品号	$n(^{206}\text{Pb})/n(^{204}\text{Pb})$		$n(^{207}\text{Pb})/n(^{204}\text{Pb})$		$n(^{208}\text{Pb})/n(^{204}\text{Pb})$		$\left[\frac{n(^{206}\text{Pb})}{n(^{204}\text{Pb})}\right]_i$	$\left[\frac{n(^{207}\text{Pb})}{n(^{204}\text{Pb})}\right]_i$	$\left[\frac{n(^{208}\text{Pb})}{n(^{204}\text{Pb})}\right]_i$
	测值	$\pm 1\sigma$	测值	$\pm 1\sigma$	测值	$\pm 1\sigma$			
FN514	17.586	0.003	15.408	0.003	38.019	0.006	17.343	15.407	37.666
FN515	17.538	0.003	15.414	0.003	38.113	0.007	17.236	15.413	37.678
FN516	17.575	0.004	15.429	0.004	38.109	0.010	17.310	15.428	37.707

注: Sr、Nd、Pb 同位素比值校正时采用义县组的锆石 U-Pb 年龄为 120 Ma, 计算公式见巫建华等, 2014。

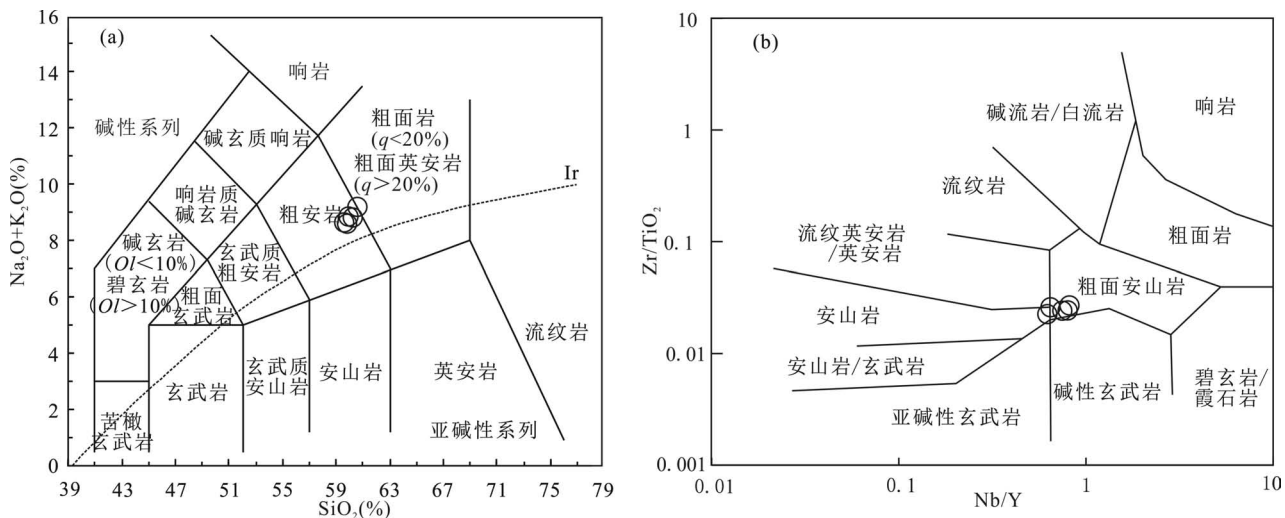


图4 冀北大滩盆地二长斑岩 TAS 图解 (a) (据 Le Bas et al., 1986) 和 Zr/TiO_2 — Nb/Y 图解 (b) (据 Winchester and Floyd, 1977)

Fig. 4 TAS (a) (after Le Bas et al., 1986) and Zr/TiO_2 — Nb/Y (b) (after Winchester and Floyd, 1977) plots of ivernite in Datan Basin, northern Hebei

石系列。在 MgO — TFeO 图解 (图 6b) 上样品点与碱性系列趋势线基本一致。可见, 样品既具有碱性系列的特征也具有钙碱性系列的特征, 属典型的钾玄武岩系列。

4.2 稀土元素

样品稀土总量较高, 变化范围为 $297 \times 10^{-6} \sim 316 \times 10^{-6}$ (平均 306×10^{-6}), 轻稀土富集明显, 变化范围

$276 \times 10^{-6} \sim 293 \times 10^{-6}$ (平均 283×10^{-6}), 重稀土变化范围 $20.8 \times 10^{-6} \sim 25.0 \times 10^{-6}$ (平均 22.7×10^{-6}), LREE/HREE 变化范围为 11.6 ~ 13.2 (平均 12.5), 稀土配分曲线图 (图 7a) 显示为右倾轻稀土富集型, $(\text{La}/\text{Yb})_N$ 变化范围为 15.5 ~ 18.6 (平均 17.4), $(\text{La}/\text{Sm})_N$ 为 4.10 ~ 4.35 (平均 4.20), $(\text{Ga}/\text{Yb})_N$ 为 2.39 ~ 2.70 (平均 2.54)。 δEu 无明显的异常,

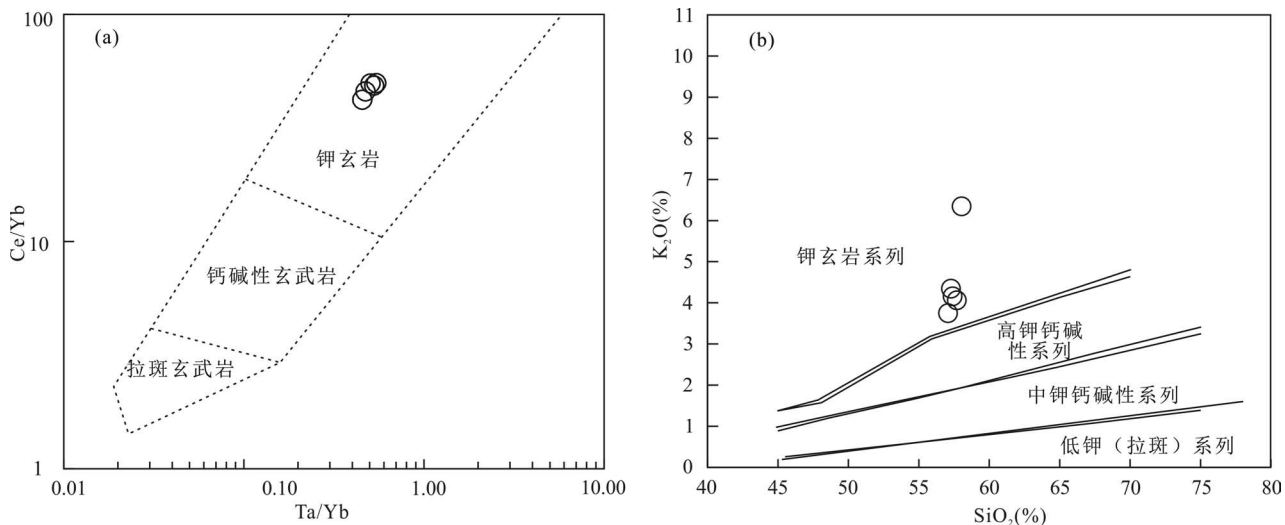


图5 冀北大滩盆地二长斑岩 Ce/Yb — Ta/Yb 图解 (a) (据 Pearce et al., 1982) 和 K_2O — SiO_2 图解 (b) (据 Peccerillo and Taylor, 1976)

Fig. 5 Ce/Yb — Ta/Yb (a) (after Pearce et al., 1982) and K_2O — SiO_2 (b) (after Peccerillo and Taylor, 1976) plots of ivernite in the Datan Basin, northern Hebei

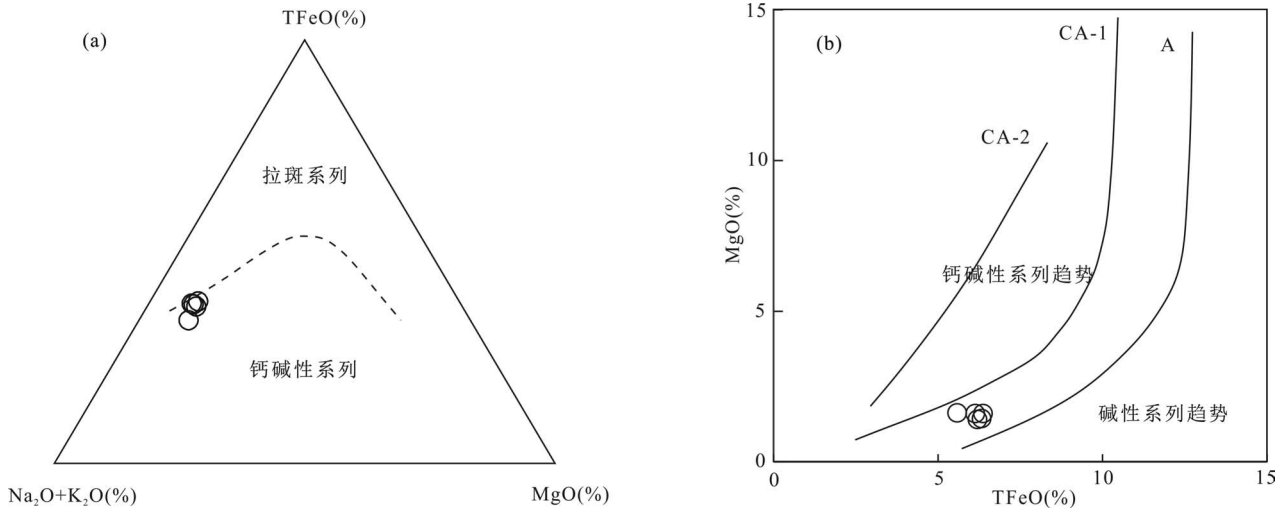


图6 冀北大滩盆地二长斑岩 AFM 图解(a) (据 Irvine et al., 1971) 和 MgO—TFeO 图解(b) (据 Morrison, 1980)
Fig. 6 AFM(a, after Irvine et al., 1971) and MgO—TFeO (b, after Morrison, 1980) plots of ivernite in Datan Basin, northern

δEu 值为 0.89~0.93, (平均 0.92); δCe 无明显的异常, δCe 值为 0.90~0.93 (平均 0.91)。

4.3 微量元素

样品大离子亲石元素(LILE) K、Rb、Ba 明显富集(图 7b), Rb 值变化范围为 $109 \times 10^{-6} \sim 189 \times 10^{-6}$ (平均 141×10^{-6}), Ba 值变化范围为 $1457 \times 10^{-6} \sim 1624 \times 10^{-6}$ (平均 1531×10^{-6}), 高场强元素(HFSE) Ta、Nb、Ti 均显示明显的负异常(图 7b)。Cr 和 Ni 的含量分别为 $1.64 \times 10^{-6} \sim 2.54 \times 10^{-6}$ (平均 1.89×10^{-6})、 $1.73 \times 10^{-6} \sim 6.51 \times 10^{-6}$ (平均 3.27×10^{-6}), 远低于原始玄武岩浆的值 $300 \times 10^{-6} \sim 500 \times 10^{-6}$ 和 300

$\times 10^{-6} \sim 400 \times 10^{-6}$ (Frey et al., 1987)。

4.4 Sr—Nd—Pb 同位素

样品的 $[n(^{87}\text{Sr})/n(^{86}\text{Sr})]_i = 0.707290 \sim 0.707399$ (平均值为 0.707343), 明显低于华北克拉通上地壳 Sr 同位素比值 ($[n(^{87}\text{Sr})/n(^{86}\text{Sr})]_i = 0.712 \sim 0.720$, Jahn et al., 1999), 明显高于亏损地幔 Sr 同位素比值 ($[n(^{87}\text{Sr})/n(^{86}\text{Sr})]_i = 0.702 \sim 0.704$, Hart, 1984), 但与华北克拉通下地壳 $\{[n(^{87}\text{Sr})/n(^{86}\text{Sr})]_i = 0.706 \sim 0.712$, Jahn et al., 1999} 的 Sr 同位素比值相近。

样品的 Nd 同位素模式年龄 $T_{\text{DM2}} = 1847 \sim$

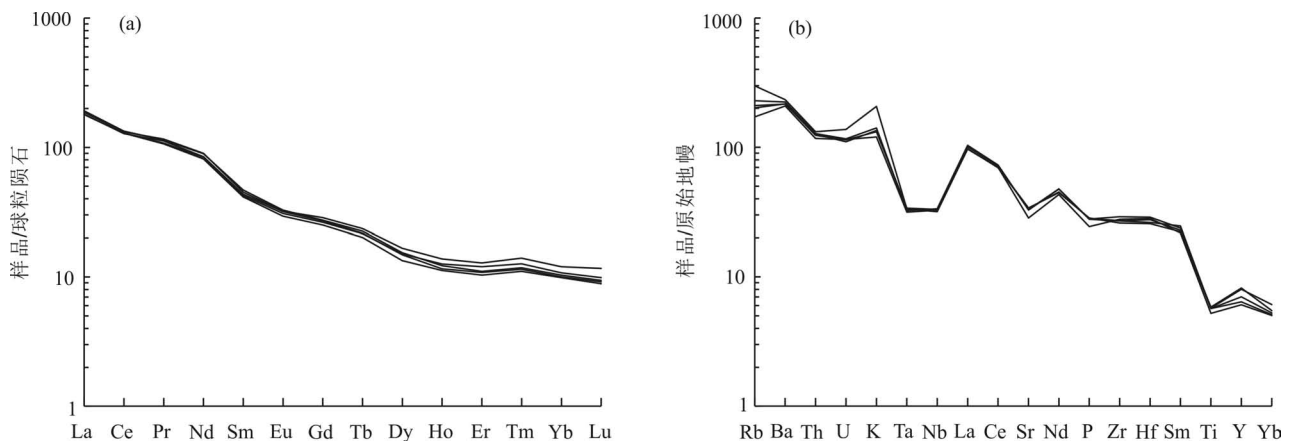


图7 冀北大滩盆地二长斑岩稀土元素球粒陨石标准化配分曲线(a)和原始地幔标准化蛛网图(b)

(球粒陨石标准化值、原始地幔标准化值据 Sun and McDonough(1989))

Fig. 7 Chondrite-normalized REE distribution patterns (a) and primitive mantel-normalized trace element spidergrams (b) of ivernite in the Datan Basin, northern Hebei (elements contents of the chondrite and primitive mantle from Sun and McDonough, 1989)

1918Ma (平均值为 1875 Ma), $[n(^{143}\text{Nd})/n(^{144}\text{Nd})]_i = 0.511849 \sim 0.511895$ (平均值为 0.511876), $\varepsilon_{\text{Nd}}(t) = -12.38 \sim -11.49$ (平均值为 -11.85), 明显高于中生代华北克拉通上地壳 ($\varepsilon_{\text{Nd}}(130\text{Ma}) \approx -25$, Liu et al., 2004) 和下地壳 ($\varepsilon_{\text{Nd}}(130\text{Ma}) \approx -33$, Liu et al., 2004) 的 $\varepsilon_{\text{Nd}}(t)$ 值, 但与富集地幔 (-13 ~ -8.0, Yang Guohui et al., 2004) 的 $\varepsilon_{\text{Nd}}(t)$ 值一致。

样品具有较低的 Pb 同位素 ($[n(^{206}\text{Pb})/n(^{204}\text{Pb})]_i = 17.236 \sim 17.343$, 平均值为 17.296、 $[n(^{207}\text{Pb})/n(^{204}\text{Pb})]_i = 15.407 \sim 15.428$, 平均值为 15.416、 $[n(^{208}\text{Pb})/n(^{204}\text{Pb})]_i = 37.666 \sim 37.707$, 平均值为 37.684), 在 Pb 同位素图解(图 9)中位于北半球铅参考线(NHRL)上方, 反映其地幔源区具有铀、钍明显富集的特征(Dupre and Allegre, 1983)。

5 岩石成因

5.1 物质来源

大滩盆地二长斑岩具有较低的 SiO_2 含量, 富集大离子亲石元素和轻稀土元素, 亏损 Nb、Ta 等高场强元素, 暗示岩浆源区有富集地幔岩石圈的贡献(Litvinovsky et al., 2002; Hollanda et al., 2006); 具有较高的 Sr ($598 \times 10^{-6} \sim 713 \times 10^{-6}$, 平均值为 $680 \times$

10^{-6}), 介于下地壳 Sr 的含量 (2900×10^{-6}) 和富集地幔 Sr 的含量 (1100×10^{-6}) 之间(Chen Bin and Zhai Mingguo, 2003), 表明岩浆可能来自于富集地幔但受到了地壳物质的影响。

大滩盆地二长斑岩 $[n(^{87}\text{Sr})/n(^{86}\text{Sr})]_i = 0.707290 \sim 0.707399$, 介于壳幔混合源区的 $[n(^{87}\text{Sr})/n(^{86}\text{Sr})]_i = 0.706 \sim 0.719$ 之间。 $\varepsilon_{\text{Nd}}(t) = -12.38 \sim -11.49$, 指示岩浆来源与地壳或富集地幔有关(邵济安等, 2010), 远高于华北克拉通古老下地壳的 $\varepsilon_{\text{Nd}}(t)$ 值 (-44 ~ -32, Jahn et al., 1999), 而与汉诺坝二辉麻粒岩包体 $\varepsilon_{\text{Nd}}(t)$ 值 (-18 ~ -8, 张国辉等, 1998) 和富集地幔 $\varepsilon_{\text{Nd}}(t)$ 值 (-13 ~ -8, Yang Guohui et al., 2004) 相似(图 8a), 表明岩浆来源与华北克拉通古老下地壳的关系较远, 而与汉诺坝二辉麻粒岩包体的源区相近, 并且与富集地幔有关。在 $[n(^{143}\text{Nd})/n(^{144}\text{Nd})]_i - [n(^{87}\text{Sr})/n(^{86}\text{Sr})]_i$ 图解(图 8b)上, 投影点靠近 EM I 富集地幔, 表明其物质来源于 EM I 富集地幔有关。在铅同位素模式 $[n(^{207}\text{Pb})/n(^{204}\text{Pb})]_i - [n(^{206}\text{Pb})/n(^{204}\text{Pb})]_i$ 图解中(图 9a), 二长斑岩的投影点落于北回归线之上的下地壳区域, 同时落在 EM I 富集地幔区域, 在 $[n(^{208}\text{Pb})/n(^{204}\text{Pb})]_i - [n(^{206}\text{Pb})/n(^{204}\text{Pb})]_i$ 图解中(图 9b), 二长斑岩的投影点落于下地壳演化线和

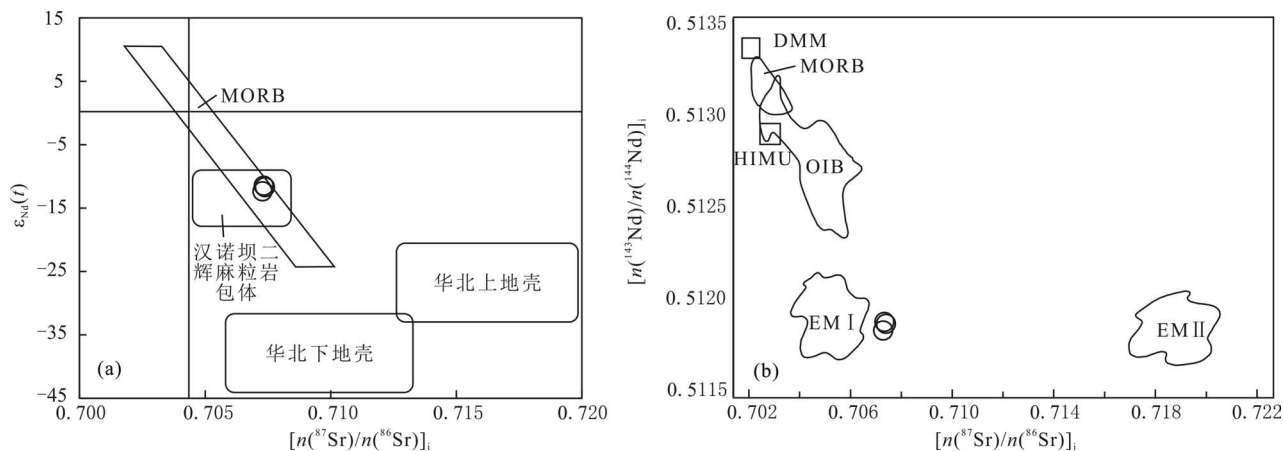


图 8 冀北大滩盆地二长斑岩 $\varepsilon_{\text{Nd}}(t) - [n(^{87}\text{Sr})/n(^{86}\text{Sr})]_i$ (a) 和 $[n(^{143}\text{Nd})/n(^{144}\text{Nd})]_i - [n(^{87}\text{Sr})/n(^{86}\text{Sr})]_i$ (b) 图解

Fig. 8 $\varepsilon_{\text{Nd}}(t) - [n(^{87}\text{Sr})/n(^{86}\text{Sr})]_i$ (a) and $[n(^{143}\text{Nd})/n(^{144}\text{Nd})]_i - [n(^{87}\text{Sr})/n(^{86}\text{Sr})]_i$ (b) plots of ivernite in Datun Basin, northern Hebei

HIMU—具有高 U/Pb 比值的地幔; MORB—洋中脊玄武岩; DMM—亏损地幔端元; EM(I、II)—富集地幔端元 (据 Zindler and Hart, 1986); NHRL—北半球参考线(据 Hart, 1984)

HIMU—mantle with high U/Pb ratio; MORB—Mid-ocean ridge basalt; EM I, EM II—enriched mantle (after Zindler and Hart, 1986); NHRL—the northern hemisphere reference line (after Hart, 1984)

汉诺坝麻粒岩的范围据张国辉等, 1998; 华北克拉通下地壳、上地壳的范围据 Jahn et al., 1999

Boundary of the granulite in Hannoba area from Zhang Guohui, 1998&; boundaries of the upper and lower crust from Jahn Bor-ming et al., 1999

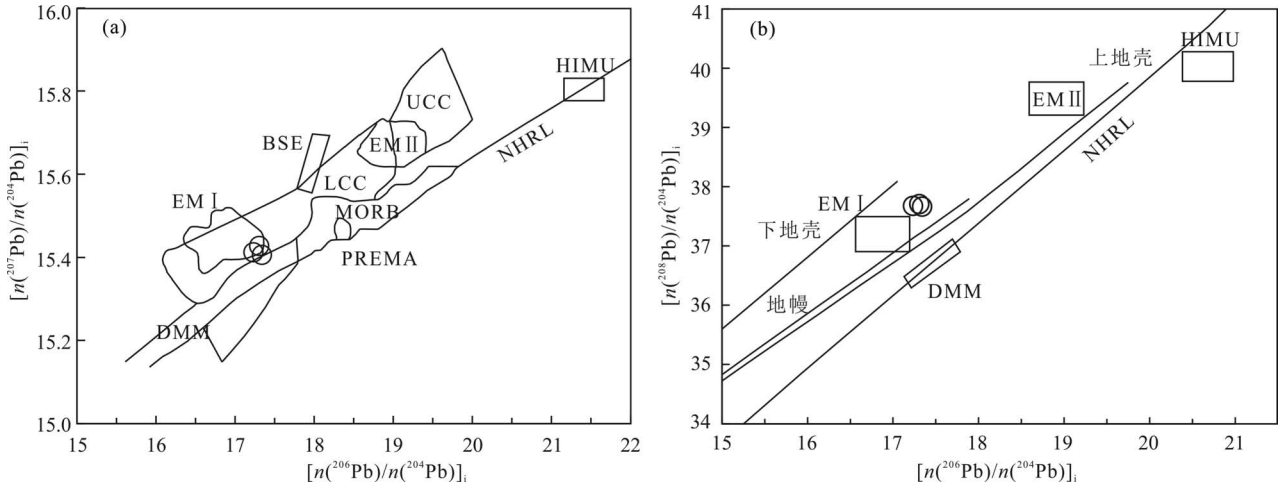


图9 冀北大滩盆地二长斑岩 $[n(^{207}\text{Pb})/n(^{204}\text{Pb})]_i$ — $[n(^{206}\text{Pb})/n(^{204}\text{Pb})]_i$ (a) 和 $[n(^{208}\text{Pb})/n(^{204}\text{Pb})]_i$ — $[n(^{206}\text{Pb})/n(^{204}\text{Pb})]_i$ (b) 图解

Fig. 9 $[n(^{207}\text{Pb})/n(^{204}\text{Pb})]_i$ — $[n(^{206}\text{Pb})/n(^{204}\text{Pb})]_i$ (a) and $[n(^{208}\text{Pb})/n(^{204}\text{Pb})]_i$ — $[n(^{206}\text{Pb})/n(^{204}\text{Pb})]_i$ (b) plots of ivernite in the Datian Basin, northern Hebei

DM—亏损地幔; EM I—I型富集地幔; PREMA—经常观测到的普通地幔; HIMU—具有高U/Pb值的地幔;

BSE—全硅酸盐地球; MORB—洋中脊玄武岩; NHRL—北半球参照线(据 Zindler and Hart, 1986)

DM—Depleted mantle; EM I—I-type enriched mantle; PREMA—Prevalent mantle; HIMU—High ratio of U/Pb mantle;

BSE—All silicate's earth; MORB—Mid-ocean ridge basalt; NHRL—Northern line of reference (after Zindler and Hart, 1986)

地幔演化线之间,同时位于EM I富集地幔区域边缘。以上特征显示二长斑岩的岩浆来源与EM I富集地幔密切相关,可能还有下地壳组分参与了大滩盆地二长斑岩的形成(邓晋福等,2006)。研究表明,汉诺坝二辉麻粒岩包体是幔源基性岩浆底侵到下地壳底部构成的年轻下地壳的一部分(樊祺诚,1996,1998,2001;张国辉等,1998),新生代时被汉诺坝玄武岩浆以包体的形式带到了地表(蔡剑辉等,2005)。这不仅说明年轻的基性麻粒岩地壳确实存在,而且为解释二长斑岩同时带有富集地幔和下地壳物质印记提供了证据。

5.2 岩浆过程

在Harker图解(图略)上,二长斑岩全岩主、微量元素与 SiO_2 的线性相关性较好,随着 SiO_2 的增高,TF FeO 、MgO、TiO₂、CaO和P₂O₅表现出明显的负相关性,而Al₂O₃和ALK表现出明显的正相关性,指示岩浆演化过程中发生铁镁质矿物(辉石、角闪石及黑云母)及钛铁矿物的结晶分异或是部分熔融时作为残留相留在源区。

5.3 构造环境

研究区所在的华北克拉通北缘隆起带中段,早白垩世早期受蒙古—鄂霍茨克以及环太平洋两大构

造体系的双重影响,形成了NE向斜列展布的火山盆地与基底隆起带相间分布的火山盆岭结构,早白垩世晚期,断陷盆地内发育伸展型碱性火山—深成岩(葛肖虹等,2014;杨文采等,2022)及热河群基性—中基性火山岩组合(或双峰式火山岩组合)(邓晋福等,1996;张宏等,2005,2006;孟凡雪等,2008;陈井胜等,2015),其中的义县组火山岩广泛分布于冀北—辽西地区,受太平洋板块俯冲的影响,区域上同样是义县组火山岩,辽西地区的火山岩有地幔来源的玄武岩(邵济安等,2005;耿显雷,2017)和俯冲带上面幔楔的局部熔融形成高镁安山岩组合(王晓蕊等,2005;洪路兵等,2017),有俯冲的洋壳部分熔融形成的镁安山岩系列组合(杨蔚,2007),也有代表下地壳部分熔融的流纹岩组合(彭艳东等,2013)。从Condie于1982年对洋俯冲带上面的岩浆弧提出的组成极性分析,空间极性反映为低K₂O的火山岩组合,和富Na的TTG组合为外弧,花岗闪长岩—花岗岩($\gamma\delta$ — γ)组合,K₂O升高的以钙碱性系列为主的火山岩系列为主弧,高K₂O的花岗岩—正长岩(γ — ξ)组合以及钾玄岩系列的火山岩为内弧(邓晋福等,2015),上述辽西地区的义县组玄武岩、高镁安山岩组合、镁安山岩组合和流纹岩组合,

均属于洋壳俯冲的外弧,即向洋一侧的外带;到了沽源—丰宁坝上地区发育的义县组钾玄岩系列,已跨过主弧,属于洋壳俯冲的内弧,对应的弧地壳厚度 $\geq 67\text{km}$,岩浆主要源于加厚陆壳底部物质的部分熔融(邓晋福等,2015),这也是研究区钾质粗安岩、粗面岩无Eu异常的原因(邓晋福等,1996)。

在用于判别钾质火成岩的构造环境判别图解中,样品落入 $\text{Zr}/\text{Al}_2\text{O}_3$ — $\text{TiO}_2/\text{Al}_2\text{O}_3$ 图(图10a)和 $\text{Ce}/\text{P}_2\text{O}_5$ — Zr/TiO_2 图(图10b)中的大陆弧(CAP)范围内,也落入 TiO_2 — Al_2O_3 图(图10c)和 Zr — Y 图(图10d)的非板内范围内,构造环境判别图解的结果可能反映出研究区二长斑岩源岩的构造环境,其大陆弧构造环境与古太平洋板块洋壳俯冲的内弧构造环境基本一致。

邓晋福等(1996)为解决燕辽燕山期火成岩安第斯式的弧火成岩特征和远离海沟的面型分布之间的矛盾,提出了“华北式(或燕辽式)造山带(大洋俯冲与岩石圈拆沉的结合)模型”。之后有众多学者从岩石学(邓晋福等,2006;熊小林等,2011;刘明启等,2018)、地球化学(许文良等,2009;何登洋等,2020)、地球物理(郭慧丽等,2014;许田等,2020)等方面进行了具体的研究。可解释为:早白垩世晚期,当太平洋板块俯冲作用顺利时,板块间的汇聚力主要被俯冲的大洋岩石圈吸收,这时对大陆地区的水平挤压力很小,可使远离海沟的燕辽地区处于中性、甚至轻微拉伸的构造环境,促使聚煤盆地的形成与火山喷发,随着大洋板块的进一步俯冲,华北东部濒太平洋地区的造山岩石圈根受到强烈的改造而变得

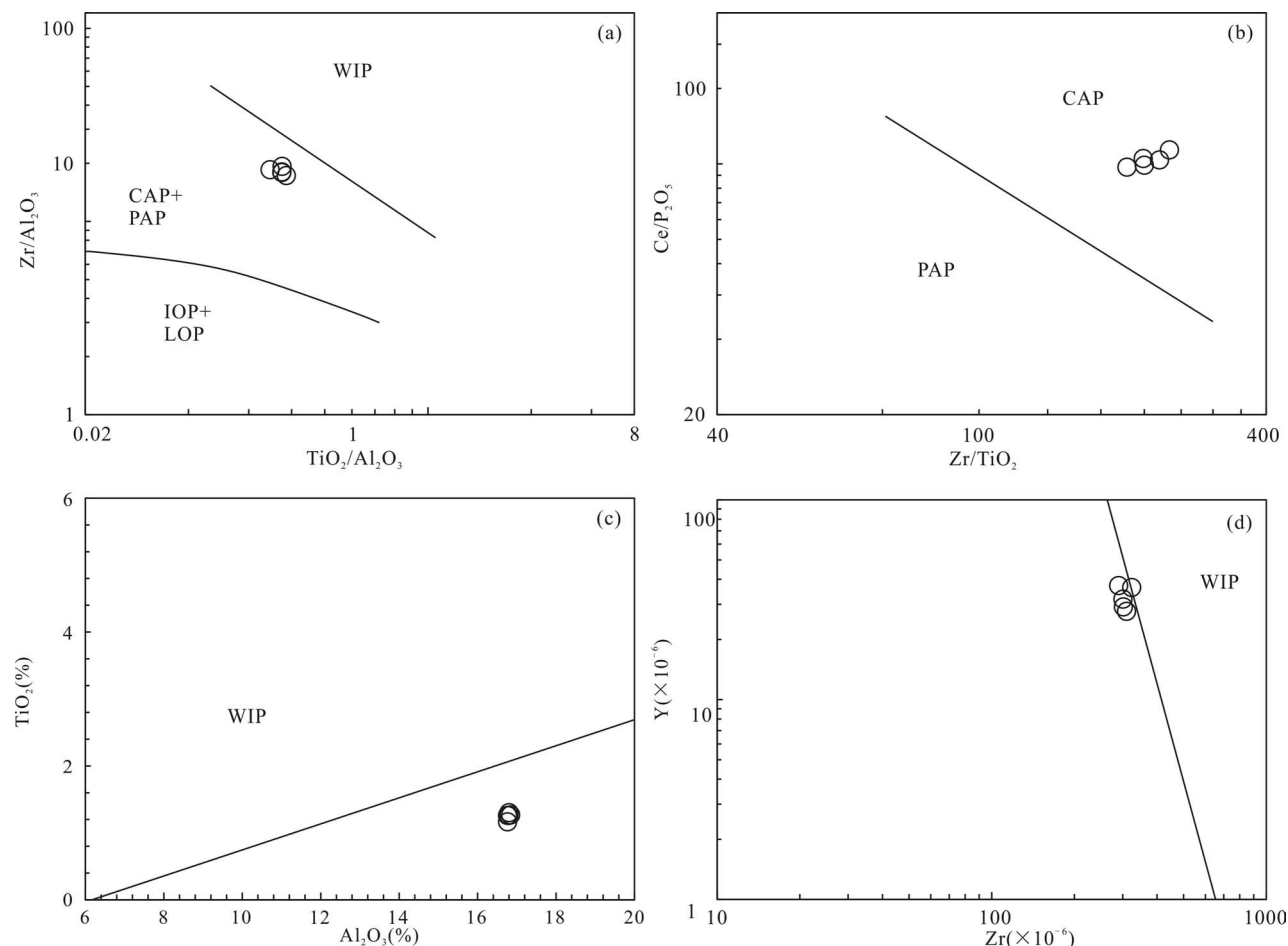


图10 冀北大滩盆地二长斑岩 $\text{Zr}/\text{Al}_2\text{O}_3$ — $\text{TiO}_2/\text{Al}_2\text{O}_3$ (a)、 $\text{Ce}/\text{P}_2\text{O}_5$ — Zr/TiO_2 (b)、 TiO_2 — Al_2O_3 (c) 和 Zr — Y (d) 图解(据 Muller and Groves, 1992)

Fig. 10 $\text{Zr}/\text{Al}_2\text{O}_3$ — $\text{TiO}_2/\text{Al}_2\text{O}_3$ (a), $\text{Ce}/\text{P}_2\text{O}_5$ — Zr/TiO_2 (b), TiO_2 — Al_2O_3 (c) and Zr — Y (d) plots of iivernite in the Datan Basin, northern Hebei (after Muller and Groves, 1992)

CAP—大陆弧; IOP—初始洋弧; LOP—晚期洋弧; PAP—后碰撞弧; WIP—板内

CAP—Continental arc; IOP—initial oceanic arc; LOP—late oceanic arc; PAP—postcollisional arc; WIP—within-plate

不稳定,造山岩石圈根由于其根带的高密度,使根带与岩石圈主体拆离而下沉,此时燕辽地区处于拉伸的构造环境,这是仍有山根(或加厚陆壳)存在的条件下地幔岩石圈减薄的结果(邓晋福等,1996,2006)。综上所述,研究区钾玄岩系列的构造环境为太平洋板块洋壳俯冲和岩石圈拆沉相结合形成的拉伸环境。

6 与铀成矿关系

在五里营二长斑岩西南部新发现的铀及多金属矿点,NE向二长斑岩岩脉、岩墙及NW向蚀变带的交点控制着该矿点深部隐伏矿体的定位,矿化强度与岩脉、岩墙及蚀变带的规模呈正相关关系,这与粤北下庄矿田“交点型”矿床成矿特征相似。矿点的矿体、异常体赋存于4条蚀变带内,以II、IV带代表。

II号带在地表由整体走向 $340^{\circ}\sim 160^{\circ}$ 的一系列硅质脉、萤石脉组成。硅质脉与整体走向 $NE20^{\circ}$ 二长斑岩脉、岩墙斜交,交角 $30^{\circ}\sim 50^{\circ}$,交点处铀含量明显增高,发育有一系列铀异常点,铀含量一般可达岩石本底值(18×10^{-6})的3~5倍,最高可达0.020%。在深部表现为厚数十米的黏土化蚀变带,局部为硅化带。在ZK5孔内表现为厚5m的硅化带,硅化带与二长斑岩交切部位发育铀异常体。IV号带呈隐伏状态,表现为厚几米至数十米的硅化、青磐岩化蚀变带。在ZK1孔表现为厚约80m的硅化、青磐岩化带。其中,硅化带与二长斑岩交切部位发育铀矿体,青磐岩化带与二长斑岩交切部位发育铅锌矿(化)体,铀矿化可分2种,一种呈红色,与微晶石英赤铁矿化关系密切;一种呈现黑色,与铅锌矿共生,与微晶石英萤石化关系密切^①。

章邦桐等(2015)对草桃背铀矿床的研究表明,其赋矿围岩橄辉玄武岩(shoshonite)以铀的带入为特征,Sr—Nd—Pb同位素示踪表明,源区经历了地幔流体的参与,对富集U等大离子亲石元素起主要制约作用。类似地,五里营铀矿点的赋矿围岩为二长斑岩,属于钾玄岩系列,分析结果显示,其铀含量达 $2.31\times 10^{-6}\sim 2.88\times 10^{-6}$,高于世界中性火成岩平均值(1.8×10^{-6} ,章邦桐等,2015),Sr—Pb—Nd同位素分析结果显示,五里营二长斑岩的形成经历了富集地幔流体的参与,促进了U、K、Rb、Ba等大离子亲石元素的富集,为铀成矿提供了地球化学方面的基本成矿条件。

7 结论

(1)大滩盆地二长斑岩全岩高钾、富碱、低钛、

贫铁,兼具碱性系列和钙碱性系列的特征,富集轻稀土元素和大离子亲石元素,无明显Eu负异常,属于钾玄岩系列。

(2)大滩盆地二长斑岩 $[n(^{87}\text{Sr})/n(^{86}\text{Sr})]_i$ 值为 $0.707290\sim 0.707399$, $[n(^{143}\text{Nd})/n(^{144}\text{Nd})]_i$ 值为 $0.511849\sim 0.511895$, $\varepsilon_{\text{Nd}}(t)$ 值变化范围是 $-12.38\sim -11.49$, $[n(^{206}\text{Pb})/n(^{204}\text{Pb})]_i$ 值为 $17.236\sim 17.343$, $[n(^{207}\text{Pb})/n(^{204}\text{Pb})]_i$ 值为 $15.407\sim 15.428$, $[n(^{208}\text{Pb})/n(^{204}\text{Pb})]_i$ 值为 $37.666\sim 37.707$ 。Sr—Nd—Pb同位素特征显示岩浆来源与EM I富集地幔密切相关,可能还有下地壳组分的参与。

(3)大滩盆地钾玄岩系列的构造环境为太平洋板块洋壳俯冲和岩石圈拆沉相结合形成的拉伸环境,岩浆主要源于加厚陆壳底部物质的部分熔融。

(4)五里营铀及多金属矿化与粤北下庄矿田“交点型”矿床成矿特征相似。赋存于一系列NNW向硅化、青磐岩化蚀变带内,钾玄岩系列火成岩与铀成矿关系密切。

致谢:参加部分野外采样工作和室内分析测试工作的还有硕士研究生夏应冰、宋凯等,章雨旭研究员和狄永军教授提出了宝贵的审稿意见,在此一并致以衷心的感谢。

参 考 文 献 / References

- (The literature whose publishing year followed by a “&” is in Chinese with English abstract; The literature whose publishing year followed by a “#” is in Chinese without English abstract)
- 鲍亦冈,白志民,葛世炜,刘澄. 1995. 北京燕山期火山地质及火山岩. 北京:地质出版社.
- 蔡剑辉,阎国翰,牟保磊,任康绪,宋彪,李凤棠. 2005. 北京房山岩体锆石 U-Pb 年龄和 Sr、Nd、Pb 同位素与微量元素特征及成因探讨. 岩石学报,21(3):776~788.
- 陈井胜,李威威,刘森,邢德和,杨佳林. 2015. 辽西建平马场义县组火山岩 LA-ICP-MS 锆石 U-Pb 年龄及其地质意义. 吉林大学学报(地球科学版),45(2):471~482.
- 邓晋福,刘厚祥,赵海玲,罗照华,郭正府,李玉文. 1996. 燕辽地区燕山期火成岩与造山模型. 现代地质,10(2):137~148.
- 邓晋福,苏尚国,刘翠,赵国春,赵兴国,周肃,吴宗. 2006. 关于华北克拉通燕山期岩石圈减薄的机制与过程的讨论:是拆沉,还是热侵蚀和化学交代? 地学前缘,13(2):105~119.
- 邓晋福,冯艳芳,狄永军,刘翠,肖庆辉,苏尚国,赵国春,孟斐,马帅,姚图. 2015. 岩浆弧火成岩构造组合与洋陆转换. 地质论评,61(3):473~485.
- 樊祺诚,刘若新. 1996. 汉诺坝玄武岩中高温麻粒岩捕虏体. 科学通报,41(3):235~238.
- 樊祺诚. 1998. 汉诺坝捕虏体麻粒岩锆石年代学与稀土元素地球化学. 科学通报,43(2):133~137.
- 樊祺诚,隋建立,刘若新,周新民. 2001. 汉诺坝榴辉岩石榴辉石

- 岩——岩浆底侵作用新证据. 岩石学报, 17(1): 1~6.
- 葛肖虹, 刘俊来, 任收麦, 袁四化. 2014. 中国东部中—新生代大陆构造的形成与演化. 中国地质, 41(1): 19~38.
- 耿显雷. 2017. 华北克拉通早白垩世义县和四合屯火山岩的地球化学和 Sr—Nd 同位素: 古老大陆下地壳物质的再循环. 导师: 高山. 武汉: 中国地质大学(武汉) 博士学位论文: 1~81.
- 郭慧丽, 徐佩芬, 张福勤. 2014. 华北克拉通及东邻西太平洋活动大陆边缘地区的 P 波速度结构: 对岩石圈减薄动力学过程的探讨. 地球物理学报, 57(7): 2352~2361.
- 何登洋, 邱昆峰, 张莲, 于皓丞, 杨泽宇. 2020. 华北克拉通兴城早白垩世玄武岩岩锆石、金红石地球化学特征及其地质意义. 岩石矿物学杂志, 39(6): 735~750.
- 贺振宇, 徐夕生, 王孝磊, 陈荣. 2008. 赣南橄榄安粗质火山岩的年代学与地球化学. 岩石学报, 24(11): 2524~2536.
- 洪路兵, 张慧慧, 任钟元, 徐义刚, 颜文. 2017. 辽西黄半吉沟早白垩世义县组高镁安山岩的成因. 岩石学报, 33(1): 41~55.
- 姜山, 潘家永, 段力, 高井明, 任伟龙, 张子龙, 王卫国. 2011. 燕山西段蔡家营—御道口断裂带的地质特征及其对铀成矿的控制作用. 东华理工大学学报(自然科学版), 34(4): 301~307.
- 黎伟, 祝洪涛, 巫建华, 吴仁贵, 张海龙, 赵博, 王常东. 2017. 内蒙古红山子—广兴铀矿田控矿因素探讨和找矿靶区优选. 东华理工大学学报(自然科学版), 40(2): 115~125.
- 李毅, 吴泰然, 罗红玲, 赵磊. 2006. 内蒙古四子王旗早白垩世钾玄岩的地球化学特征及其形成构造环境. 岩石学报, 22(11): 2791~2800.
- 廖群安, 邱家骧. 1993. 北京地区中生代钾玄岩系列—高钾钙碱性系列的识别和成因分析. 岩石学报, 9(增刊): 14~23.
- 廖群安, 王京名, 薛重生, 李昌年. 1999. 江西广丰白垩世盆地中两类玄武岩的特征及其与盆地演化的关系. 岩石学报, 15(1): 116~123.
- 刘明启, 李忠海. 2018. 克拉通岩石圈减薄与破坏机制的动力学数值模拟. 中国科学: 地球科学, 48(7): 844~877.
- 孟凡雪, 高山, 柳小明. 2008. 辽西凌源地区义县组火山岩锆石 U-Pb 年代学和地球化学特征. 地质通报, 27(3): 364~373.
- 孟艳宁, 范洪海, 陈东欢, 王生云. 2015. 河北省涿源地区 460 矿床的铀矿矿物学特征研究. 东华理工大学学报(自然科学版), 38(4): 335~343.
- 彭艳东, 黄菲, 邢德和, 张志斌. 2013. 辽西建平义县组火山岩形成构造环境的地球化学鉴别. 东北大学学报(自然科学版), 34(7): 1012~1016.
- 邱家骧, 林景任. 1991. 岩石化学. 北京: 地质出版社: 95~111.
- 邵济安, 路凤香, 张履桥, 杨进辉. 2005. 辽西义县组玄武岩捕虏晶的发现及其意义. 岩石学报, 21(6): 1547~1558.
- 邵济安, 牟保磊, 朱慧忠, 张履桥. 2010. 大兴安岭中南段中生代成矿物质的深部来源与背景. 岩石学报, 26(3): 649~656.
- 宋凯, 巫建华, 牛子良, 吴仁贵, 刘帅. 2017. 冀北多本沟盆地流纹岩年代学、地球化学特征及地质意义. 东华理工大学学报(自然科学版), 40(4): 323~333.
- 王佳玲, 巫建华. 2014. 赣东北晚白垩世橄榄玄粗岩系列火山岩中单斜辉石矿物化学及其地质意义. 岩石矿物学杂志, 33(1): 163~173.
- 王晓蕊, 高山, 柳小明, 袁洪林, 胡兆初, 张宏, 王选策. 2005. 辽西四合屯早白垩世义县组高镁安山岩的地球化学: 对下地壳拆沉作用和 Sr/Y 变化的指示. 中国科学(D 辑: 地球科学), 35(8): 700~709.
- 巫建华, 武珺, 祝洪涛, 郭国林, 吴仁贵, 刘帅, 余达淦. 2013. 大兴安岭红山子盆地火山岩系岩石地层对比. 高校地质学报, 19(3): 472~483.
- 巫建华, 项媛馨, 钟志菲. 2014a. 江西广丰、玉山盆地橄榄玄粗岩的 SHRIMP 锆石 U-Pb 定年和 Sr—Nd—Pb—O 元素同位素特征. 岩石矿物学杂志, 33(4): 645~656.
- 巫建华, 解开瑞, 吴仁贵, 郭国林, 刘帅. 2014b. 中国东部中生代流纹岩—粗面岩组合与热液型铀矿研究新进展. 地球科学进展, 29(12): 1372~1382.
- 巫建华, 丁辉, 牛子良, 吴仁贵, 祝民强, 郭国林, 刘帅, 余达淦. 2015. 河北涿源张麻井铀—钼矿床围岩 SHRIMP 锆石 U-Pb 定年及其地质意义. 矿床地质, 34(4): 757~768.
- 巫建华, 解开瑞, 祝洪涛, 吴仁贵, 刘帅. 2016. 大兴安岭南端红山子盆地流纹岩的成因: 元素和 Sr—Nd—Pb 同位素制约. 吉林大学学报(地球科学版), 46(6): 1724~1739.
- 巫建华, 张婧妍, 姜山, 解开瑞, 郭国林, 吴仁贵. 2017a. 冀北涿源铀矿田粗面岩的年代学、地球化学特征及岩石成因. 地球化学, 46(2): 105~122.
- 巫建华, 郭国林, 郭佳磊, 张旗, 吴仁贵, 余达淦. 2017b. 中国东部中生代岩浆岩的时空分布及其与热液型铀矿的关系. 岩石学报, 33(5): 1591~1614.
- 吴俊奇, 谭桂丽, 章邦桐, 凌洪飞, 陈培荣. 2011. 赣中早白垩世橄榄玄粗岩(Shoshonite)系列火山岩的厘定及成因研究. 高校地质学报, 17(4): 479~491.
- 夏应冰, 巫建华, 姜山, 吴仁贵, 刘帅. 2016. 冀北大滩盆地粗面岩的年代学、地球化学特征及成因研究. 高校地质学报, 22(4): 608~620.
- 项媛馨, 巫建华, 余达淦, 刘帅. 2012. 赣东北晚白垩世橄榄玄粗岩(Shoshonite)系列火山岩厘定的地质证据. 东华理工大学学报(自然科学版), 35(1): 43~53.
- 解开瑞, 巫建华, 祝洪涛, 吴仁贵, 刘帅. 2016. 大兴安岭南端芝瑞盆地流纹岩年代学、地球化学及岩石成因. 地球化学, 45(3): 249~267.
- 熊小林, 刘星成, 朱志敏, 李元肖, 万生, 宋茂双, 张生, 吴金花. 2011. 华北埃达克质岩与克拉通破坏: 实验岩石学和地球化学依据. 中国科学: 地球科学, 41(5): 654~667.
- 许田, 黄金水. 2020. 华北地区重力和地形及其对克拉通破坏深部过程的约束. 大地测量与地球动力学, 40(5): 517~521.
- 许文良, 孙德有, 周燕. 1994. 满洲里—绥芬河地学断面岩浆作用和地壳结构. 北京: 地质出版社.
- 许文良, 杨德彬, 裴福萍, 王枫, 王微. 2009. 华北克拉通中生代拆沉陆壳物质对岩石圈地幔的改造: 来自橄榄岩捕虏体中角闪石的成分制约. 吉林大学学报(地球科学版), 39(4): 606~617.
- 薛怀民, 陶奎元. 1989. 宁芜地区中生代火山岩系列的新认识及其地质意义. 江苏地质, (11): 9~14.
- 薛怀民, 马芳, 曹光跃. 2015. 长江中下游地区晚中生代橄榄玄粗岩系列火山岩: 年代学格架、地球化学特征及成因讨论. 地质学报, 89(8): 1380~1401.
- 杨蔚. 2007. 辽西中生代火山岩年代学及地球化学研究——对华北克拉通岩石圈减薄机制的制约. 导师: 李曙光. 合肥: 中国科学技术大学博士学位论文: 1~123.
- 杨文采. 2022. 中—新生代东北和华北的洋陆转换作用. 地质论评, 68(3): 770~780.
- 章邦桐, 吴俊奇, 凌洪飞, 陈培荣. 2008. 会昌早白垩世橄榄玄粗岩(shoshonite)成因的元素及 Sr—O—Nd—Pb 同位素地球化学证据. 地质学报, 82(7): 986~997.
- 章邦桐, 吴俊奇, 凌洪飞, 陈培荣. 2011a. 关于 Shoshonite 中译名的商榷和建议. 地质论评, 57(2): 216~217.
- 章邦桐, 吴俊奇, 凌洪飞, 陈培荣. 2011b. 板内橄榄玄粗岩(shoshonite)地幔流体交代作用及成因的元素地球化学证据: 以赣南会昌橄榄玄粗岩为例. 地球化学, 40(5): 443~453.

- 张国辉,周新华,孙敏,陈绍海,冯家麟. 1998. 河北汉诺坝玄武岩中麻粒岩类和辉石岩类俘虏体 Sr、Nd、Pb 同位素特征及其地质意义. *岩石学报*,14(2):190~197.
- 张宏,柳小明,陈文,李之彤,杨芳林. 2005. 辽西北票—义县地区义县组顶部层位的年龄及其意义. *中国地质*,32(4):596~603.
- 张宏,柳小明,袁洪林,胡兆初,第五春荣. 2006. 辽西凌源地区义县组下部层位的 U-Pb 测年及意义. *地质论评*,2006,52(1):63~71.
- 张双涛,吴泰然,许绚,Byamba J, Amarjargal A, 王时麒,李忠权. 2005. 内蒙古中部早白垩世钾玄岩的发现及其意义. *北京大学学报(自然科学版)*,41(2):212~218.
- 张雅菲,巫建华,姜山,刘玄,吴仁贵,刘帅,郭国林. 2016. 冀北大滩盆地轴(钼)成矿流纹岩—花岗斑岩 SHRIMP 锆石 U-Pb 定年、地球化学及 Sr—Nd 同位素特征. *岩石学报*,32(1):193~211.
- 张运涛,裴荣富,于波,陈永飞,杨东生,邱小平. 2013. 草桃背矿床白垩纪橄榄玄粗岩与轴成矿关系. *吉林大学学报(地球科学版)*,43(5):1423~1435.
- 周万蓬. 2015. 相山地区岩浆演化及其对轴成矿作用的制约. 导师:范洪海,郭福生. 北京:核工业北京地质研究院博士学位论文:1~160.
- 朱凤丽. 2012. 河北省涿源县大官厂轴钼矿床围岩蚀变与成矿. *东华理工大学学报(自然科学版)*,35(1):30~37.
- 祝洪涛,李继木,赵博,王常东. 2014. 大兴安岭红山子盆地轴钼矿勘查新进展及其找矿意义. *东华理工大学学报(自然科学版)*,37(4):360~366.
- 祝禧艳,巫建华. 2007. 赣南晚侏罗世橄榄玄粗岩系列的发现. *东华理工大学学报(自然科学版)*,30(2):125~131.
- Bao Yigang, Bai Zhigang, Ge Shiwei, Liu Deng. 1995#. *Yanshanian volcanic geology and volcanic rocks in Beijing*. Beijing: Geological Press.
- Cai Jianhui, Yan Guohan, Mou Baolei, Ren Kangxu, Song Biao, Li Fengshang. 2005&. Zircon U-Pb age, Sr—Nd—Pb isotopic compositions and trace element of Fangshan complex in Beijing and their petrogenesis significance. *Acta Petrologica Sinica*,21(3):776~788.
- Chen Bin and Zhai Mingguo. 2003. Geochemistry of late Mesozoic lamprophyre dykes from the Taihang Mountains, north China, and implications for the sub-continental lithospheric mantle. *Geological Magazine*,140(2):87~93.
- Chen Jingsheng, Li Weiwei, Liu Miao, Xing Dehe, Yang Jialin. 2015&. U-Pb isotopic age of the volcanic rocks of the Yixian Formation in Jianping Machang of western Liaoning and its geological significance. *Journal of Jilin University (Earth Science Edition)*,45(2):471~482.
- Condie K C. 1986. 板块构造与地壳演化(1982,第二版). 杜宽平,等. 译. 武汉:武汉地质学院:1~326.
- Deng Jinfu, Liu Houxiang, Zhao Hailin, Luo Zhaohua, Guo Zhengfu, Li Yuwen. 1996&. Yanshanian igneous rocks and oroceny model, *Geoscience*,10(2):137~148.
- Deng Jinfu, Su Shanguo, Liu Cui, Zhao Guochun, Zhao Xingguo, Zhou Su, Wu Zong. 2006&. Discussion on the lithospheric thinning of the North China craton: delamination? or thermal erosion and chemical metasomatism? *Earth Science Frontiers*,13(2):105~119.
- Deng Jinfu, Feng Yangfang, Di Yongjun, Liu Cui, Xiao Guoqing, Su Shanguo, Zhao Guochun, Meng Fei, Ma Shuai, Yao Tu. 2015&. Magmatic arc and ocean—continent transition: discussion. *Geological Review*,61(3):473~485.
- Dupre B, Allegre C J. 1983. Pb—Sr isotopic variation in Indian Ocean basalts and mixing phenomena. *Nature*,303:142~146.
- Fan Qicheng, Liu Ruoxin. 1996#. Hannuoba basalt medium—high temperature granulite capture body. *Chinese Science Bulletin*,41(3):235~238.
- Fan Qicheng. 1998#. Zircon chronology and REE geochemistry of granulite xenolith at Hannuoba. *Chinese Science Bulletin*,43(2):133~137.
- Fan Qicheng, Sui Jianli, Liu Ruoxin, Zhou Xinmin. 2001&. Eclogite facies garnet—pyroxenolite xenolith in Hannuoba area; New evidence of magma underplatin. *Acta Petrologica Sinica*,17(1):1~6.
- Frey F A, Green D H. 1978. Integrated models of basalt Petrogenesis: A study of quartzite to olivine melilitites from south eastern Australia utilizing geochemical and experimental petrological data. *Journal of Petrology*,19:463~513.
- Ge Xiaohong, Liu Junlai, Ren Shoumai, Yuan Sihua. 2014&. The formation and evolution of the Mesozoic—Cenozoic continental tectonics in eastern China. *Geology in China*,41(1):19~38.
- Geng Xianlei. 2017&. Geochemical and Sr—Nd isotopic compositions of Early Cretaceous Yixian and Sihetun lavas from the North China Craton: Recycling of ancient lower. Tutor: Gaoshan. Wuhan: Doctoral dissertation of China University of Geosciences (Wuhan):1~81.
- Guo HuiLi, Xu Peifen, Zhang Fuqin. 2014&. Pwave velocity structure of the North China Craton and west pacific active continental margin: exploration for dynamic processes of lithospheric thinning. *Chinese Journal of Geophysics*,57(7):2352~2361.
- Hart S R. 1984. A large scale isotope anomaly in the Southern Hemisphere mantle. *Nature*,309:753~757.
- He Dengyang, Qiu Kunfeng, Zhang Lian, Yu Haocheng, Yang ZeYu. 2020&. Zircon and rutile geochemistry of the Early Cretaceous basaltic porphyry from Xingcheng in the North China Craton and its geodynamic implications. *Acta Petrologica et Mineralogica*,39(6):735~750.
- He Zhenyu, Xu Xisheng, Wang Xiaolei, Chen Rong. 2008&. Geochronology and geochemistry of shoshonitic volcanics in southern Jiangxi Province. *Acta Petrologica Sinica*,24(11):2524~2536.
- Hollanda M H B M, Pimentel M M, Oliveira D C, Jardim de Sád E F. 2006. Lithosphere—asthenosphere interaction and the origin of Cretaceous tholeiitic magmatism in Northeastern Brazil; Sr—Nd—Pb isotopic evidence. *Lithos*,86(1):34~49.
- Hong Lubing, Zhang Yinhu, Ren Zhongyuan, Xu Yigang. 2017&. Petrogenesis of Huangbanjigou high magensium andesite in Early Cretaceous Yixian Formation, western Liaoning. *Acta Petrologica Sinica*,33(1):41~55.
- Humphris S E, Thompson G. 1978. Trace element mobility during hydrothermal alteration of oceanic basalts. *Geochimica Et Cosmochimica Acta*,42(1):127~136.
- Irvine T N, Baragar R A. 1971. A guide to the chemical classification of the common volcanic rocks. *Journal of Earth Sciences*,8:523~548.
- Jahn B M, Wu Fuyuan, Lo C H, Chin H T. 1999. Crust—mantle interaction induced by deep subduction of the continental crust: geochemical and Sr—Nd isotropic evidence from post-collisional mafic—ultramafic intrusion of the northern Dabie complex, central China. *Chemical Geology*,157(1):119~146.
- Jiangshan, Pan Jiayuan, Duan Li, Gao Jingming, Ren Weilong, Zhang Zilong, Wang Weiguo. 2011&. Geologic features of Caijiaying—Yudaokou fracture zone in the western Yanshan Mt. and its control role on uranium mineralization. *Journal of East China Institute of*

- Technology(Natural Science Edition),34(4):301~307.
- John R N, Alan J W, Philip L B. 2002. Porphyry gold—copper mineralization in the Cadia district, eastern Lachlan Fold Belt, New South Wales and its relationship to shoshonitic magmatism. *Mineralium Deposits*,37:100~116.
- Le Bas M J, Le Maitre R W, Streckeisen A, Zanettin B. 1986. A chemical classification of volcanic rocks based on the total alkali—silica diagram. *Journal of Petrology*,27(3):745~750.
- Li Wei, Zhu Hongtao, Wu Jianhua, Wu Rengui, Zhang Hailong, Zhao Bo, Wang Changdong. 2017&. Discussion on ore controlling factors and the validation of optimal prospecting target area in Hongshanzi—Guangxing uranium ore-field Inner Mongolia. *Journal of East China Institute of Technology (Natural Science Edition)*, 40(2):115~125.
- Li Yi, Wu Tairan, Luo Hongling, Zhaolei. 2006&. Geochemistry and tectonic setting of the early Cretaceous shoshonite of Siziwangqi area, Inner Mongolia. *Acta Petrologica Sinica*,22(11):2791~2800.
- Liao Qunan, Qiu Jiaxiang. 1993. Identification and genetic analysis of the Mesozoic shoborgite series—high-potassium calc-alkaline series in Beijing area. *Acta Petrologica Sinica*,9(s):14~23.
- Liao Qunan, Wang Jingming, Xue Chongsheng, Li Changnian. 1999&. The characteristics of two kinds basalts in Cretaceous basin and thier relations with the basin's evolution, in Shangrao—Guangfeng district, Jiangxi province. *Acta Petrologica Sinica*, 15(1):116~123.
- Liegeois J P, Navez J, Hertogen J, Black R. 1998. Contrasting origin of post-collisional high-K calc-alkaline and shoshonitic versus alkaline and peralkaline granitoids. The use of sliding normalization. *Lithos*, 45:1~28.
- Litvinovsky B A, Jahn B M, Zandvilevich A N, Shadaeva M G. 2002. Crystal fractionation in the petrogenesis of an alkali monzodiorite—syenite series; the Oshurkovo plutonic sheeted complex, Transbaikalia, Russia. *Lithos*,64:97~130.
- Liu Yongsheng, Gao Shan, Yuan Hongling, Zhou Lian, Liu Xiaoming, Wang Xuance, Hu Zhaochu, Wang Linsen. 2004. U-Pb zircon ages and Nd, Sr, and Pb isotopes of lower crustal xenoliths from North China Craton; insights on evolution of lower continental crust. *Chemical Geology*,211(1):87~109.
- Liu Mingqi, Li Zhonghai. 2018&. Dynamics of thinning and destruction of the continental cratonic lithosphere: Numerical modeling. *Science China Earth Sciences*,48(7):844~877.
- Meng Fanxue, Gao Shan, Liu Xiaoming. 2008&. U-Pb zircon geochronology and geochemistry of volcanic rocks of the Yixian Formation in the Lingyuan area, western Liaoning, China. *Geological Bulletin of China*,27(3):364~373.
- Meng Yanning, Fan Honghai, Chen Donghuan, Wang Yunsheng. 2015&. Mineralogical characters of No. 460 deposit in Guyuan area, Hebei Province. *Journal of East China Institute of Technology (Natural Science Edition)*,38(4):335~343.
- Morrison G W. 1980. Characteristics and tectonic setting of the Shoshonite rock association. *Lithos*,13(1):97~108
- Muller D, Roek N M S, Croves D L. 1992. Geochemical discrimination between shoshonitic and potassic volcanic rocks in different tectonic settings: A pilot study. *Mineralogy and Petrology*,46:259~289.
- Pearce J A. 1982. Trace element characteristics of lavas from destructive plate boundaries. In: Thorpe R s. ed. *Andesites, Orogenic Andesites and Related Rocks*. New York: John Wiley & Sons,525~548.
- Peccerillo A, Taylor S R. 1976. Geochemistry of eocene calc-alkaline volcanic rocks from the Kastamonu area, Northern Turkey. *Contributions to Mineralogy and Petrology*,58(1):63~81
- Peccerillo A. 1999. Multiple mantle metasomatism in central—southern Italy. *Geochemical effects, timing and geodynamic implication. Geology*,27(4):315~318.
- Peccerillo A. 2001. Geochemistry and petrogenesis of Quaternary magmatism in Central—southern Italy. *Geochemistry International*, 39(6):521~535.
- Peng Yandong, Huang Fei, Xing Dehe, Zhang Zhibin. 2013&. Geochemical discrimination of tectonic environments of volcanic rocks of Yixian Formation in Jianping of western Liaoning. *Journal of Northeastern University(Natural Science)*,34(7):1012~1016.
- Rollinson H R. 1993. *Using geochemical data: Evaluation, presentation, interpretation*. Singapore: Longman Scientific and Technical:1~352.
- Shao Ji'an, Lu Fengxiang, Zhang Lvqiao, Yang Jinhui. 2005&. Discovery of xenocrysts in basalts of Yixian Formation in west Liaoning Province and its significance. *Acta Petrologica Sinica*,21(6):1547~1558.
- Shao Ji'an, Mu Baolei, Zhu Huizhong, Zhang Lvqiao. 2010&. Material source and tectonic settings of the Mesozoic mineralization of the Da Hinggan Mts. *Acta Petrologica Sinica*,26(3):649~656.
- Song Kai, Wu Jianhua, Nu Ziliang, Wu Rengui, Liu Shuai. 2017&. Geochronology, geochemical characteristics and its geological implications of the rhyolite of the Duobengou basin in Weichang, Hebei Province. *Journal of East China Institute of Technology (Natural Science Edition)*,40(4):323~333.
- Sun C H and Stern R J. 2001. Genesis of Mariana shoshonites: contribution of the subduction component. *Journal of Geophysical Research*,106:589~608.
- Sun S S, McDonough W F. 1989. Chemical and isotopic systematics of oceanic basalts; implications for mantle composition and processes. In: Saunders AD and Norry MJ(eds.). *Magmatism in the Ocean Basins*. Geological Society, London, Special Publications, 42(1):313~345.
- Thompson R N. 1985. Asthenospheric source of Ugandan ultrapotassic magma. *Geol.*,93:603~608.
- Varne R. 1985. Ancient subcontinental mantle: A source for K-rich orogenic volcanics. *Geology*,23:405~408.
- Wang Jialing, Wu Jianhua. 2014&. Mineral chemistry of clinopyroxenes from the Late Cretaceous shoshonitic volcanic rocks in Northern Jiangxi Province and its geological significance. *Acta Petrologica et Mineralogica*,33(1):163~173.
- Wang Xiaoren, Gao Shan, Liu Xiaoming, Yuan Honglin, Hu Zhaochu, Zhang Hong, Wang Xuance. 2005#. Geochemistry of high-magnesium andesites from the Early Cretaceous Yixian Formation in Sihetun, Western Liaoning; An indication of lower crustal delamination and Sr/Y changes. *Science China: Earth Sciences*,35(8):700~709.
- Winchester J A, Floyd P A. 1976. Geochemical magma type discrimination: application to altered and metamorphosed basic igneous rocks. *Earth and Planet Sci Let*,28:459~469
- Wu Jianhua, Wu Jun, Zhu Hongtao, Guo Guolin, Wu Rengui, Liu Shuai, Yu Dagan. 2013&. Lithostratigraphical correlation of the volcanic rock series in Hongshanzi basin in Great Hingan Range. *Geological Journal of China Universities*,19(3):472~483.
- Wu Jianhua, Xiang Yuanxin, Zhong Zhifei. 2014a&. SHRIMP zircon U-Pb dating and Sr—Nd—Pb—O isotope characteristics of shoshonite

- from Guangfeng and Yushan basins in Jiangxi Province. *Acta Petrologica et Mineralogica*, 33(4):645~656.
- Wu Jianhua, Xie Kairui, Wu Rengui, Guo Guolin, Liu Shuai. 2014b&. The new progress in the study of Mesozoic rhyolite—trachyte assemblage and hydrothermal-type Uranium Mineralization in Eastern China. *Advances in Earth Science*, 29(12):1372~1382.
- Wu Jianhua, Niu Ziliang, Wu Rengui, Zhu Minqiang, Guo Guolin, Liu Shuai, Yu Dagan. 2015&. SHRIMP zircon U—Pb dating of country rock in Zhangmajing U—Mo deposit in Guyuan, Hebei Province, and its geological significance. *Mineral Deposits*, 34(4):757~768.
- Wu Jianhua, Xie Kairui, Zhu Hongtao, Wu Rengui, Liu Shuai. 2016&. Petrogenesis of rhyolite from Hongshanzi basin in southern Greater Xing'an Range: elements and Sr—Nd—Pb isotope constraints. *Journal of Jilin University (Earth Science Edition)*, 46(6):1724~1739.
- Wu Jianhua, Zhang Jingyan, Jiang Shan, Xie Kairui, Guo Guolin, Wu Rengui. 2017a&. Geochronology, geochemical characteristics and petrogenesis of trachytes in the Guyuan uranium ore field, northern Hebei Province. *Geochimica*, 46(2):105~122.
- Wu Jianhua, Guo Guolin, Guo Jialei, Zhang Qi, Wu Rengui, Yu Dagan. 2017b&. Spatial—temporal distribution of Mesozoic igneous rock and their relationship with hydrothermal uranium deposits in eastern China. *Acta Petrologica Sinica*, 33(5):1591~1614.
- Wu Junqi, Tan Guili, Zhang Bangtong, Ling Hongfei, Chen Peirong. 2011&. Identification and genesis of the Early Cretaceous shoshonitic volcanic rock series in central Jiangxi Province. *Geological Journal of China Universities*, 17(4):479~491.
- Xia Yingbing, Wu Jian, Jiang Shan, Wu Rengui, Liu Shuai. 2016&. Geochronology, geochemical characteristics, and genesis of trachyte in Datan basin, northern Hebei. *Geological Journal of China Universities*, 22(4):608~620.
- Xiang Yuanxin, Wu Jianhua, Yu Dagan, Liu Shuai. 2012&. Shoshonite series volcanic rocks in northern Jiangxi Province. *Journal of East China Institute of Technology (Natural Science Edition)*, 35(1):43~53.
- Xie Kairui, Wu Jianhua, Zhu Hongtao, Wu Rengui, Liu Shuai. 2016&. Petrogenesis of early Late Jurassic rhyolites from the Zhirui Basin in southern Daxing'an Range: Their chronologic and geochemical constrains. *Geochimica*, 45(3):249~267.
- Xiong Xiaolin, Liu Xingcheng, Zhu Zhimin, Li Yuanxiao, Wan Sheng, Song Maoshuang, Zhang Sheng, Wu Jinhua. 2011&. Adakitic rocks and destruction of the North China Craton; Evidence from experimental petrology and geochemistry. *Sci China Earth Sci*, 41(5):654~667.
- Xu Tian, Huang Jinshui. 2020&. Constraints of gravity and topography on the destruction of North China Craton. *Journal of Geodesy and Geodynamics*. *Journal of Geodesy and Geodynamics*, 40(5):517~521.
- Xu Wenliang, Sun Deyou, Zhou Yan. 1994#. *Manzhouli—Suifenhe Geoscience Section Magmatism and Crustal Structure*. Beijing: Geological Press.
- Xu Wenliang, Yang Debin, Pei Fuping, Wang Fengg, Wang Wei. 2009&. Mesozoic lithospheric mantle modified by delaminated lower continental crust in the North China Craton: Constraints from compositions of amphiboles from peridotite xenoliths. *Journal of Jilin University (Earth Science Edition)*, 39(4):606~617.
- Xue Huaimin, Tao Kuiyuan. 1989#. New understanding of Mesozoic volcanic rock series in Ningwu area and its geological significance. *Jiangsu Geology*, (11):9~14.
- Xue Huaimin, Ma Fang, Cao Guangyue. 2015&. Late Mesozoic shoshonitic volcanic rocks in the middle and lower Yangtze River reaches: ages, geochemical and genesis. *Acta Geologica Sinica*, 89(8):1380~1401.
- Yang Jinhui, Sun Linchung, Zhai Mingguo, Zhou Xinhua. 2004. Geochemical and Sr—Nd—Pb isotopic compositions of mafic dikes from the Jiaodong Peninsula, China: evidence for vein-plus-peridotite melting in the lithospheric mantle. *Lithosphere*, 73(3~4):145~160.
- Yang Wei. 2007&. *Chronology and Geochemistry of Mesozoic Volcanic Rocks in Western Liaoning: Constraints on the Mechanism of Lithospheric Thinning in the North China Craton*. Tutor: Li Shuguang. Hefei: Doctoral dissertation of University of Science and Technology of China: 1~123.
- Yang Wencai. 2022&. Ocean—continent transition process revealed by worldwide comparison of crust and upper mantle structures. *Geological Review*, 68(3):770~780.
- Zhang Bangtong, Wu Junqi, Ling Hongfei, Chen Peirong. 2008&. Geochemical evidence of element and Sr—O—Nd—Pb isotopes for petrogenesis of the Huichang Early Cretaceous shoshonite, southern Jiangxi province. *Acta Geologica Sinica*, 82(7):986~997.
- Zhang Bangtong, Wu Qunqi, Ling Hongfei, Chen Peirong 2011a&. An arguement and a suggestion an the chinese name for Shoshonite. *Geological Review*, 57(2):216~217.
- Zhang Bangtong, Wu Junqi, Ling Hongfei, Chen Peirong. 2011b&. Elemental geochemical evidence for genesis of intraplate shoshonite and mantle-derived fluid metasomatism: shoshonite from Huichang, southern Jiangxi Province as an example. *Geochimica*, 40(5):443~453.
- Zhang Guohui, Zhou Xinhua, Sun Min, Chen Shaohai, Feng Jialin. 1998&. Sr, Nd and Pb isotopic characteristics of granulite and pyroxenite xenoliths in Hannuoba basalts, Hebei Province, and their implication for geologic processes. *Acta Petrologica Sinica*, 14(2):190~197.
- Zhang Hong, Liu Xiaoming, Chen Wen, Li Zhitong, Yang Fanglin. 2005&. The age of the top of the Yixian Formation in the Beipiao—Yixian area, western Liaoning, and its importance. *Geology in China*, 32(4):596~603.
- Zhang Hong, Liu Xiaoming, Yuan Honglin, Hu Zhaochu, Diwu Chunrong. 2006&. U—Pb isotopic age of the lower Yixian Formation in Lingyuan of western Liaoning and its significance. *Geological Review*, 2006, 52(1):63~71.
- Zhang Shuangtao, Wu Tairan, Xu Xun, Byamba J, Amarjargal A, Wang Shilin, Li Zhongquan. 2005&. The significance of discovery of Early Cretaceous shoshonite in central Inner Mongolia. *Acta Scientiarum Naturalium*, 41(2):212~218.
- Zhang Shuanhong, Zhao Yue, Ye Hao, Liu Jianming. 2014. Origin and evolution of the Bainaimiao arc belt: Implications for crustal growth in the southern Central Asian orogenic belt. *Geological Society of America Bulletin*, 126(9~10):1275~1300.
- Zhang Yafei, Wu Jianhua, Jiang Shan, Liu Xuan, Wu Rengui, Liu Shuai, Guo Guolin. 2016&. SHRIMP U—Pb geochronology, geochemistry and Sr—Nd isotopes of the uranium—(molybdenum) related rhyolite and granitic porphyry, Datan, northern Hebei. *Acta Petrologica Sinica*, 32(1):193~211.
- Zhang Yuntao, Pei Rongfu, Yu Bo, Chen Yonfei, Yang Dongsheng, Qiu Xiaoping. 2013&. Relation between Cretaceous shoshonite and

uranium metallogenesis in Caotaobei uranium deposit. *Journal of Jilin University (Earth Science Edition)*, 43(5):1423~1435.

Zhou Wanpeng. 2015. The Magmatic Evolution in Xianshang Area and its Important Role in the Uranium Mineralization. Tutor: Fan Honghai, Guo Fusheng. Beijing: Doctoral dissertation of Beijing Research Institute of Uranium Geology: 1~160.

Zhu Fengli. 2012. Rock alteration and mineralization of Daguanchang uran-molybdate deposit in Guyuan Country, Hebei Province. *Journal of East China Institute of Technology (Natural Science Edition)*, 35(1):30~37.

Zhu Hongtao, Li Jimu, Zhao Bo, Wang Changdong. 2014. Exploration progress of Hongshanzi basin in Daxinganling and its prospecting significance. *Journal of East China Institute of Technology (Natural Science Edition)*, 37(4):360~366.

Zhu Xiyan, Wu Jianhua. 2007. The discovery of Late Jurassic shoshonitic rocks in south Jiangxi. *Journal of East China Institute of Technology (Natural Science Edition)*, 30(2):125~131.

Zindler Aand Hart S R. 1986. Chemical geodynamics. *Annual Reviews of Earth and Planetary Sciences*, 14:493~571.

Determination, petrogenesis and relationship with uranium mineralization of shoshonite series in Datan Basin, northern Hebei

GAO Tiandong¹⁾, GUO Hengfei¹⁾, JIANG Shan¹⁾, Wu Jianhua²⁾, NIU Ziliang¹⁾,
WANG Hongzhi¹⁾, WANG Zhisheng¹⁾, MA Guoxiang¹⁾

1) No. 243 Geological Party of Nuclear Industry, CNNC, Chifeng, Inner Mongolia, 024006;

2) State Key Laboratory of Nuclear Resources and Environment, East China University of Technology, Nanchang, 330013

Objectives: The Datan basin is situated in the uplift belt of the northern margin of the North China Craton and the southwest section of the Guyuan—Hongshanzi uranium metallogenic belt. A number of uranium occurrences and uranium anomaly site have been newly discovered in the Wuliying area of the basin. They mainly occurs in the middle—basic subvolcanic rocks of the Yixian period, and the geological age belongs to the late Early Cretaceous, which is obviously different from the known ore-bearing horizons in this metallogenic belt—the Zhangjiakou Formation high-potassium calc-alkaline rhyolite in the early Early Cretaceous. The rock—alkaline trachyte assemblage and the high-potassium calc-alkaline—alkaline rhyolite assemblage of the Xinmin Formation in the early Late Jurassic. However, there is still a lack of systematic research on lithology, petrography, geochemical characteristics and petrogenesis in this ore-bearing layer.

Methods: Based on detailed observations of occurrence of Wuliying uranium occurrences in the field, we have studied the petrology, geochemistry, Sr—Nd—Pb radio isotope of host rocks to discuss nature of source region and tectonic setting, than, we have discussed the relationship between middle—basic subvolcanic rocks and uranium mineralization.

Results: The host rock is ivernite. All of ivernites are characterized by high contents of K_2O and total alkali, low contents of TiO_2 and iron, and an enrichment of LREE and LILE element. It has the characteristics of alkaline series and calc alkaline series, and belongs to the typical shoshonite series. $[n(^{87}Sr)/n(^{86}Sr)]_i$ between 0.707290 and 0.707399 (the average is 0.707343), $[n(^{143}Nd)/n(^{144}Nd)]_i$ between 0.511849 and 0.511895 (the average is 0.511876), $\epsilon_{Nd}(t)$ range of $-12.38 \sim -11.49$, $[n(^{206}Pb)/n(^{204}Pb)]_i$ between 17.236 and 17.343 (the average is 17.296), $[n(^{207}Pb)/n(^{204}Pb)]_i$ between 15.407 and 15.428 (the average is 15.416), $[n(^{208}Pb)/n(^{204}Pb)]_i$ between 37.666 and 37.707 (the average is 37.684). In the $\epsilon_{Nd}(t)$ — $[n(^{87}Sr)/n(^{86}Sr)]_i$, $[n(^{143}Nd)/n(^{144}Nd)]_i$ — $[n(^{87}Sr)/n(^{86}Sr)]_i$, $[n(^{207}Pb)/n(^{204}Pb)]_i$ — $[n(^{206}Pb)/n(^{204}Pb)]_i$, and $[n(^{208}Pb)/n(^{204}Pb)]_i$ — $[n(^{206}Pb)/n(^{204}Pb)]_i$ diagrams.

Conclusions: The ivernite belongs to the typical shoshonite series, which shows the source of magma is closely related to EM I enriched mantle, and possibly the participation of lower crust components. Simultaneously, affected by the subduction of the oceanic crust of the Pacific plate and the delamination of the North China Craton's lithosphere, its tectonic environment is a tensile environment, and the magma mainly originates from the partial melting of the material at the bottom of the thickened continental crust. The Wuliying uranium mineralization is

similar to the "junction type" uranium deposit in the Xiazhuang orefield. Uranium mineralization occurs in a series of NNW-trending silicification and cyanidation alteration zones, and The enriched mantle imprint of its host rock, iavernite (shoshonite series), restricts the enrichment of LILE such as U.

Keywords: shoshonite series; EM I enriched mantle; tectonic environment; uranium mineralization; Datan basin

First author: GAO Tiandong, male; born in 1967, senior engineer, research in uranium geological production

Manuscript received on: 2022-03-16; Accepted on: 2022-08-11; Network published on: 2022-08-20

Doi: 10.16509/j.georeview.2022.08.045

Edited by: ZHANG Yuxu

